Starshades 101

N. Jeremy Kasdin
Princeton University

Stuart Shaklan
Jet Propulsion Laboratory, California Institute of Technology

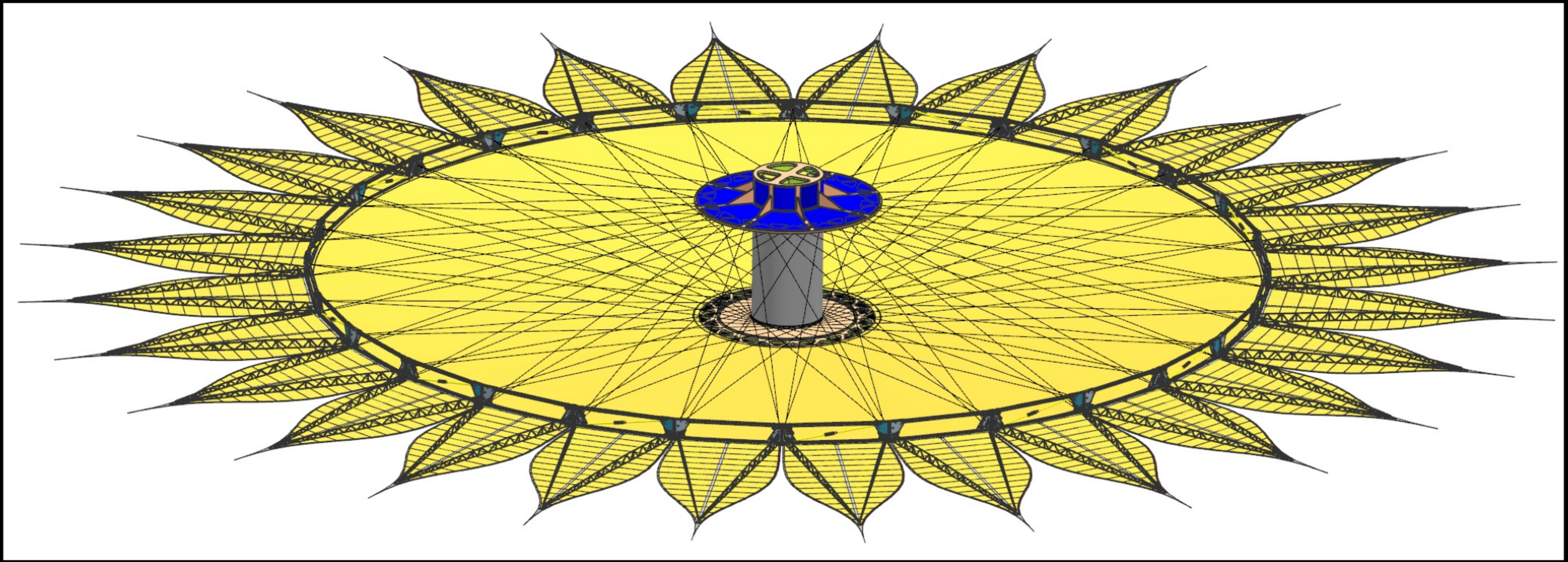

Government sponsorship acknowledged

Outline

- Starshade Design
- Making it Work
- Operational Considerations

Nature's Starshade


July 11, 1991


August 11, 1999

Create an artificial eclipse to block out sunlight, place telescope in resulting shadow.

Simple Ray Optics Description

A solid, circular occulter of radius R.

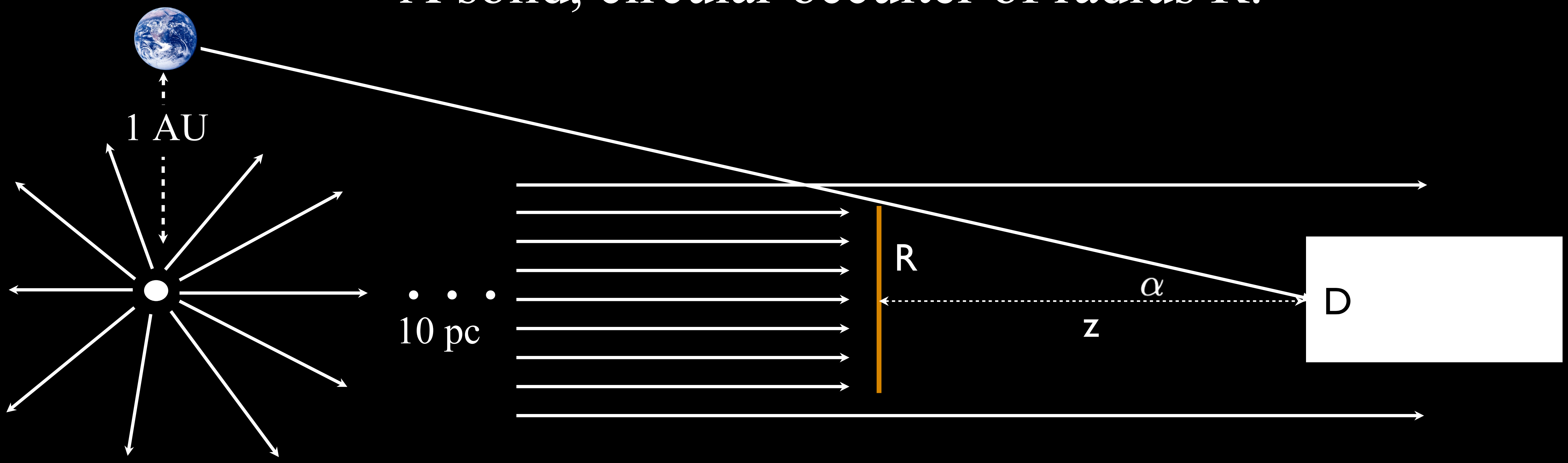

IWA = α = angle to tip of starshade
= R/Z

A 6m dia. disk at 6,000 km separation gives access to 1AU at 10 parsec

First proposed by Lyman Spitzer in 1962

Why use a starshade?

- Immune to telescope errors
- Operates in broadband
- Maximizes throughput
- No outer working angle limitation
- Inner working angle set by geometry

Main limitation is the number of observations, determined by fuel and mission time.

However, as with a coronagraph, we have to consider diffraction . . . .

Diffracted field around circular disk

Allowing for diffraction, shadow no darker than 1e-3.

Shadow (linear scale)

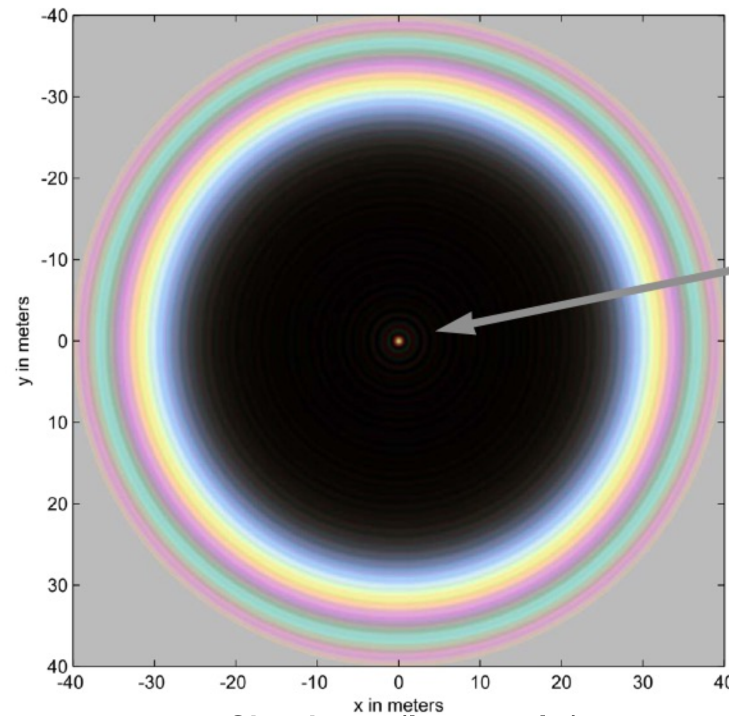

Poisson's Spot!

Circular Occulter

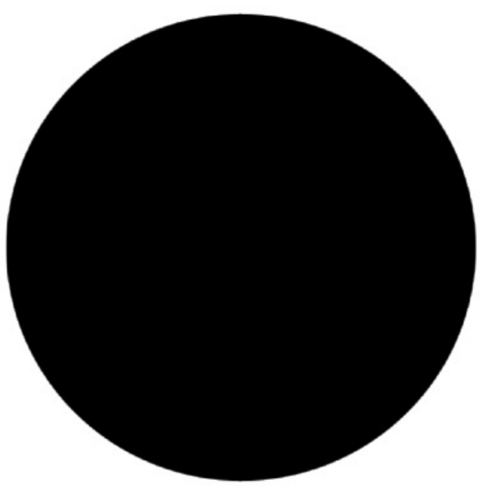

Shadow (log scale)

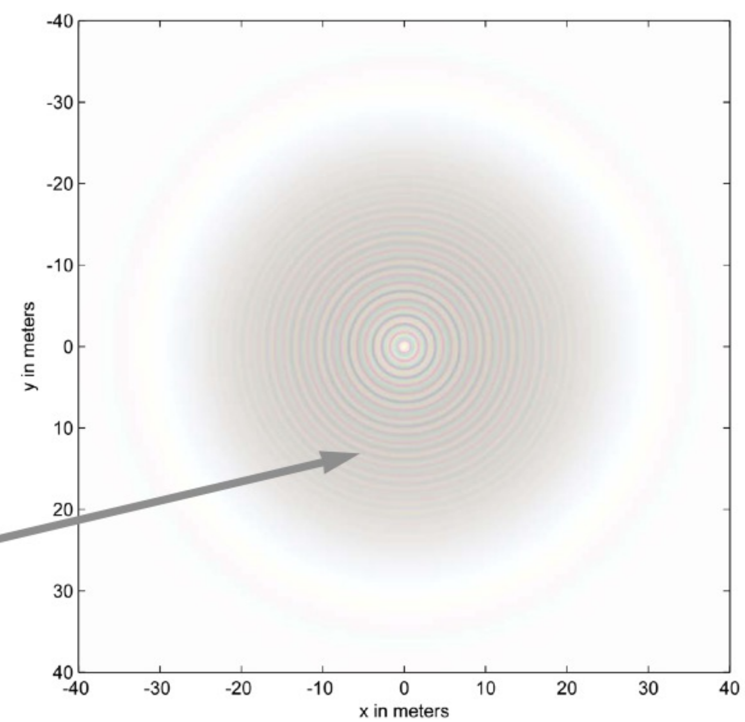

Shadow isn't dark enough

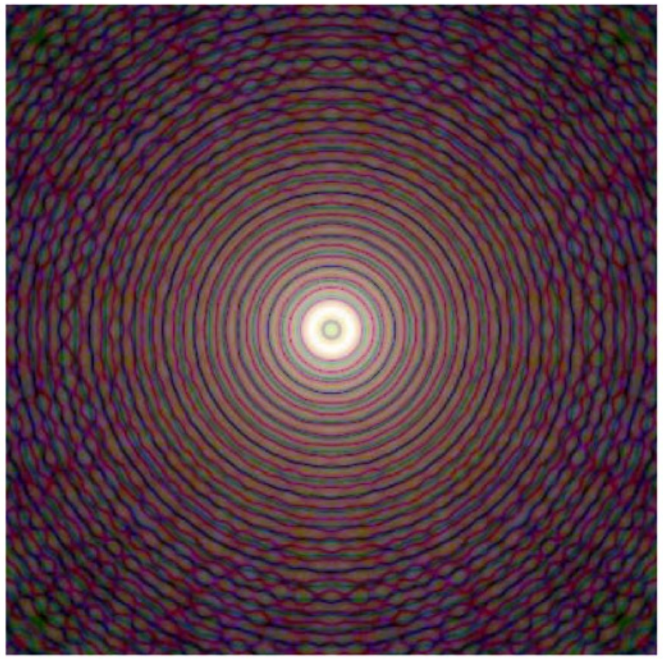

Simulated star/planet image

Solving for Diffraction

Babinet's Principle (linearity)

$$E_{starshade}(r) = 1 - E_{hole}(r)$$

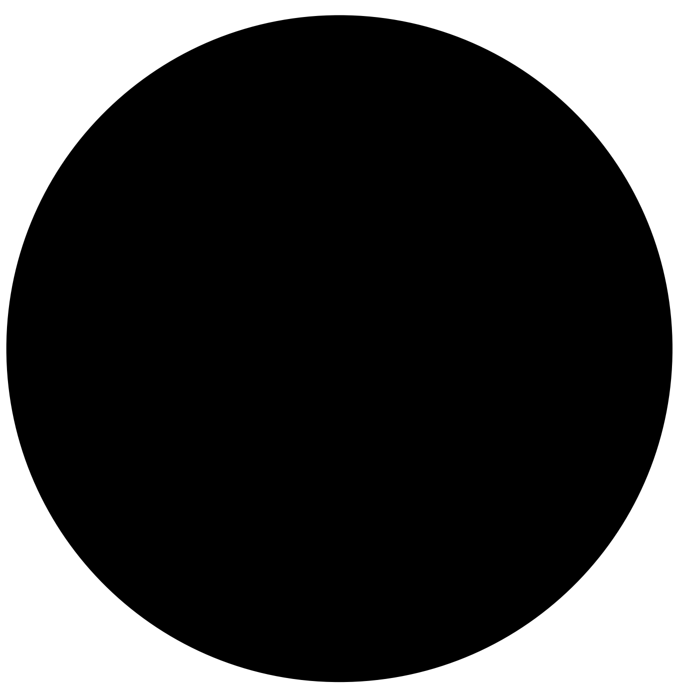

= 1 -

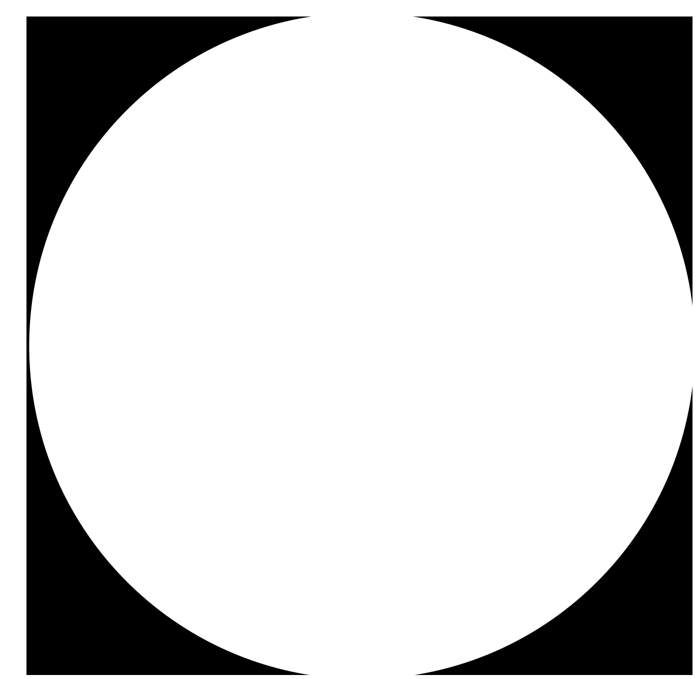

$$E_{hole}(\rho) = \frac{2\pi}{i\lambda z} e^{\frac{i\pi}{\lambda z}\rho^2} \int_0^R e^{\frac{i\pi}{\lambda z} r^2} J_0\left(\frac{2\pi r \rho}{\lambda z}\right) r\,dr$$

Fresnel Transform

To achieve 10^{-10} suppression, a circular occulter would need to be roughly 750 times larger and 750 times further away than ray optics solution to control diffraction.

So, the question becomes, how to design a starshade that is smaller and closer while achieving the same high suppression and small inner working angle.

Apodize the Occulter

It has been known since 1962 (Spitzer) that an apodized occulter can produce the needed shadow.

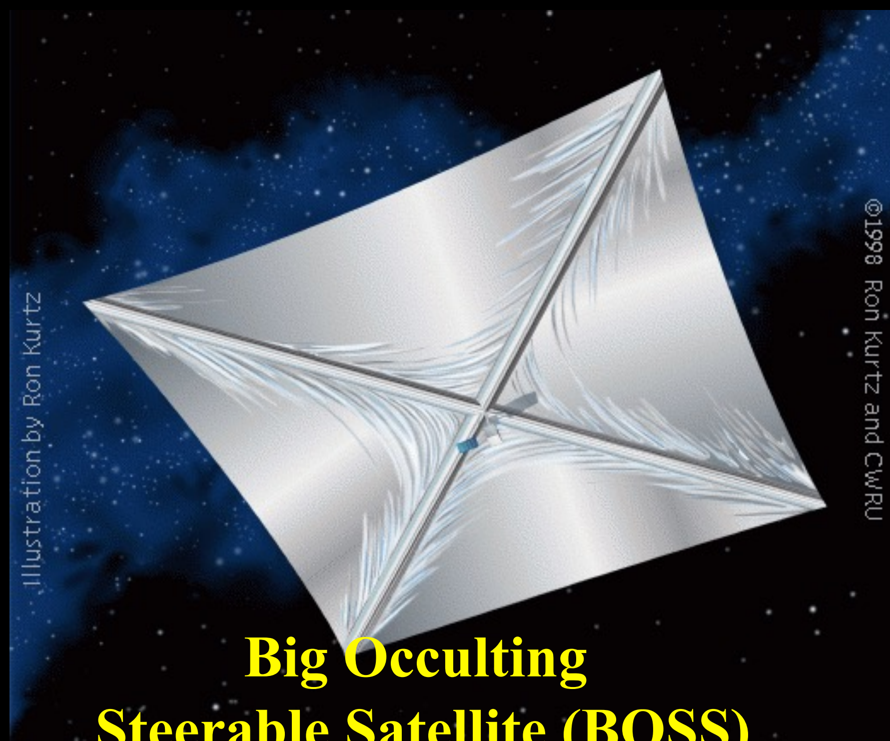

Copi & Starkman (2000)

Schultz (2003)

$$E(\rho) = E_0 e^{\frac{2\pi i z}{\lambda}} \left(1 - \frac{2\pi}{i\lambda z} e^{\frac{i\pi}{\lambda z}\rho^2} \int_0^R A(r) e^{\frac{i\pi}{\lambda z} r^2} J_0 \left(\frac{2\pi r \rho}{\lambda z} \right) r dr \right)$$

Smoothly vary transmission by *A(r)*

Apodize the Occulter

It has been known since 1962 (Spitzer) that an apodized occulter can produce the needed shadow.

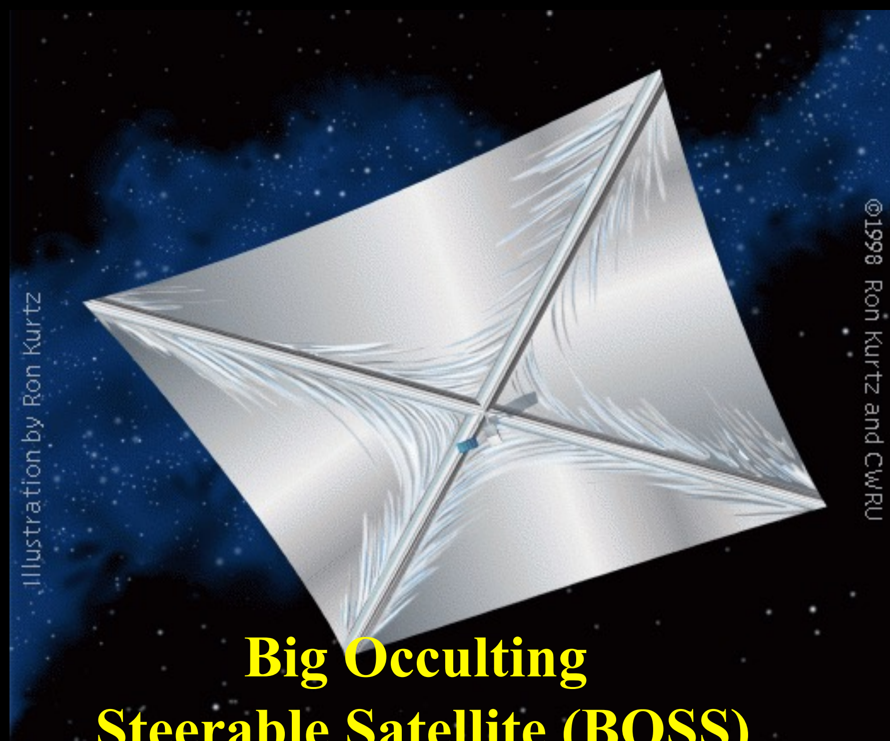

Copi & Starkman (2000)

Schultz (2003)

$$E(\rho) = E_0 e^{\frac{2\pi i z}{\lambda}} \left(1 - \frac{2\pi}{i\lambda z} e^{\frac{i\pi}{\lambda z}\rho^2} \int_0^R A(r) e^{\frac{i\pi}{\lambda z} r^2} J_0\left(\frac{2\pi r \rho}{\lambda z}\right) r dr\right)$$

Smoothly vary transmission by *A(r)*

Apodize the Occulter

It has been known since 1962 (Spitzer) that an apodized occulter can produce the needed shadow.

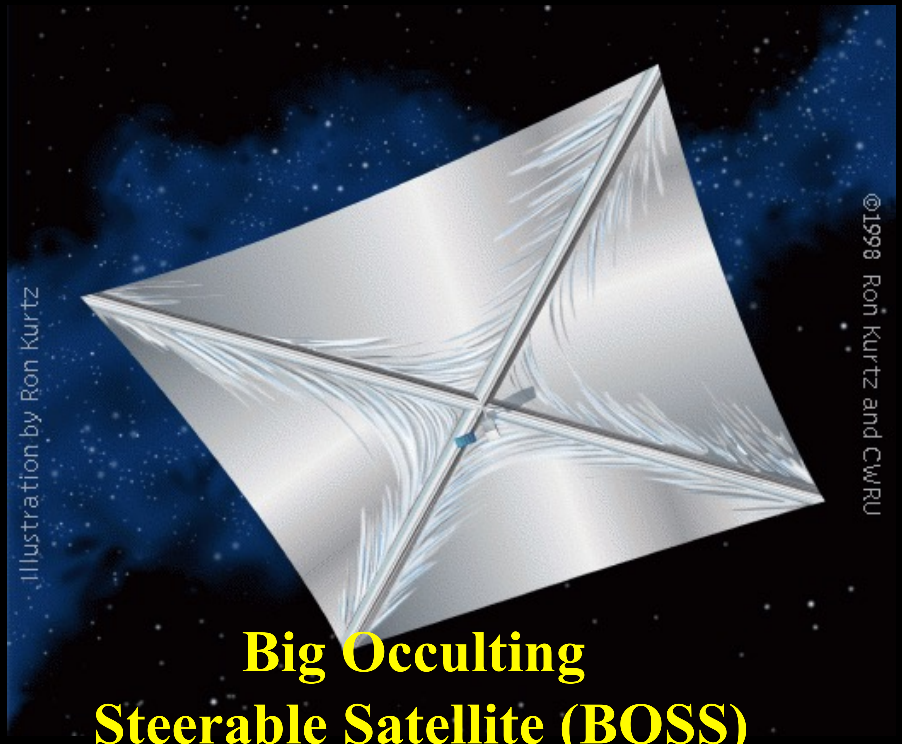

Copi & Starkman (2000)

Schultz (2003)

$$E(\rho) = E_0 e^{\frac{2\pi i z}{\lambda}} \left(1 - \frac{2\pi}{i\lambda z} e^{\frac{i\pi}{\lambda z}\rho^2} \int_0^R A(r) e^{\frac{i\pi}{\lambda z} r^2} J_0\left(\frac{2\pi r \rho}{\lambda z} \right) r dr \right)$$

Smoothly vary transmission by *A(r)*

Optimal Apodization

Vanderbei, et al. (2007) solved a linear program to find apodization at discrete points along radius using exact, scalar integral.

* Electric field suppression
* Shadow diameter
* Inner Working Angle
* Shortest wavelength of bandpass
* Longest wavelength of bandpass
* Smoothness
* Engineering features (gaps and tip widths)

→ Global minimum establishes size, distance, shape of occulter

The increased degrees of freedom allow for smaller occulter design and flexibility to achieve constraints such as larger gaps, petal length, or wider tips.

Convert apodization to binary occulter

Uses same approach as star-shaped pupil design.

Marchal (1985), Simmons (2005), Cash (2006), Vanderbei et al. (2007)

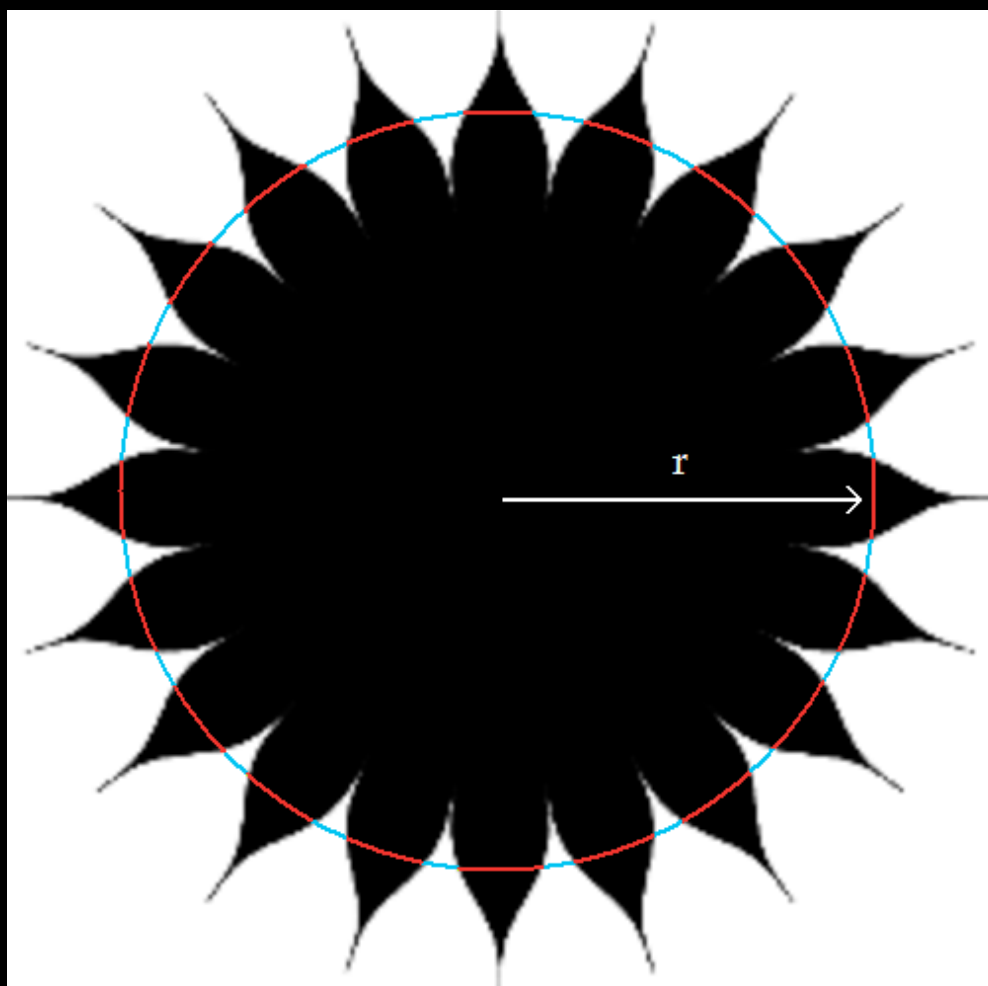

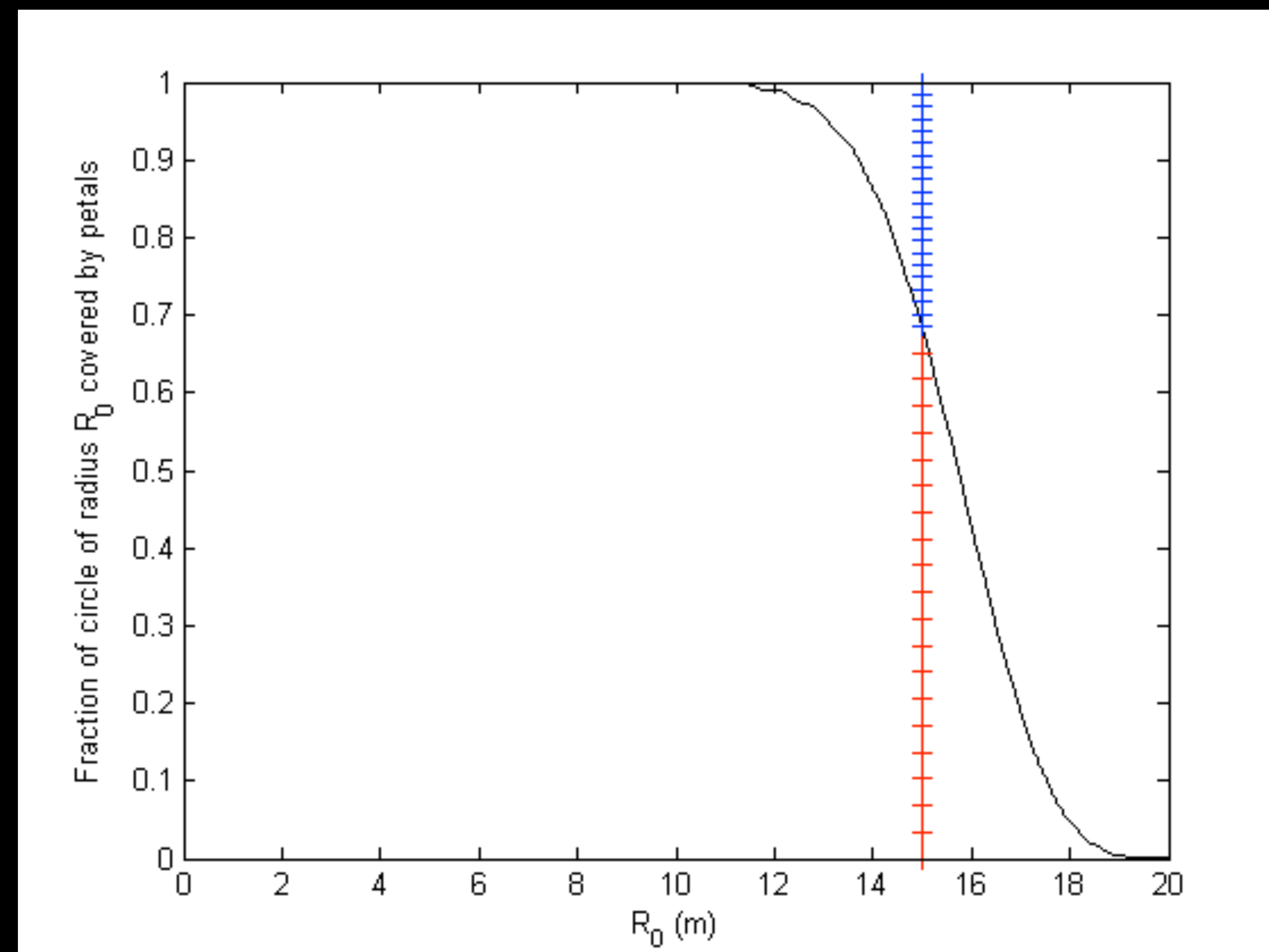

$$
\begin{aligned}
E_{o,\mathrm{petal}}(\rho,\phi) \;=\;& E_{o,\mathrm{apod}}(\rho) \\
& -E_0 e^{\frac{2\pi i z}{\lambda}} \sum_{j=1}^{\infty} \frac{2\pi(-1)^j}{i\lambda z} \left(\int_0^R e^{\frac{\pi i}{\lambda z}(r^2+\rho^2)} J_{jN}\left(\frac{2\pi r \rho}{\lambda z}\right) \frac{\sin\left(j\pi A(r)\right)}{j\pi} r\,dr \right) \\
& \quad \times \left(2\cos\left(jN(\phi-\pi/2)\right)\right)
\end{aligned}
$$

Shaped Occulter

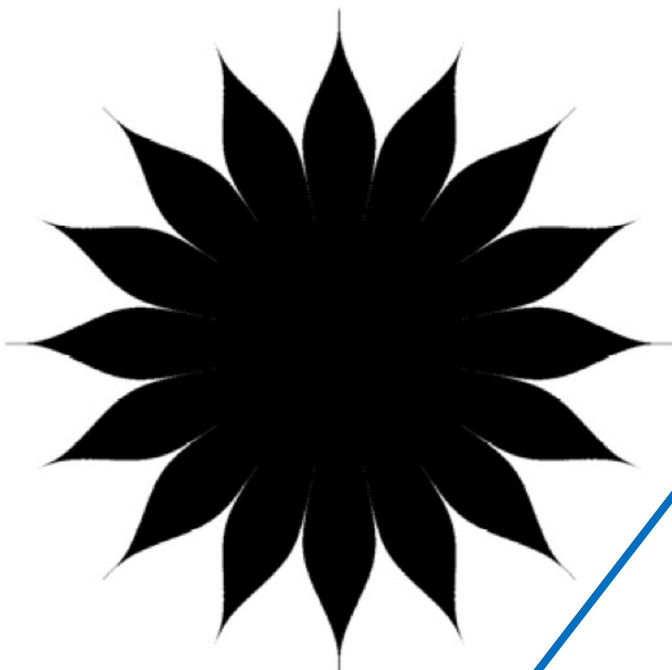

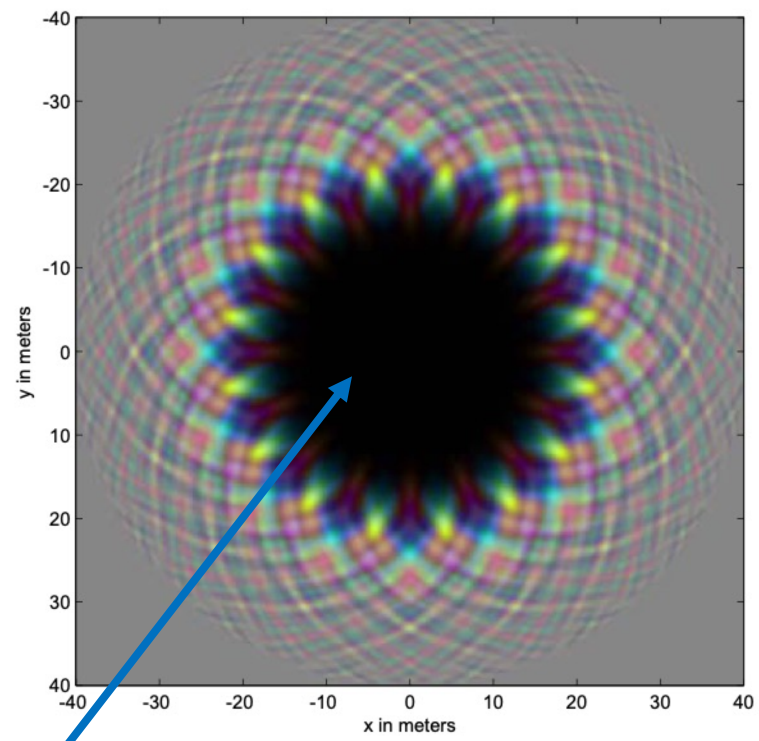

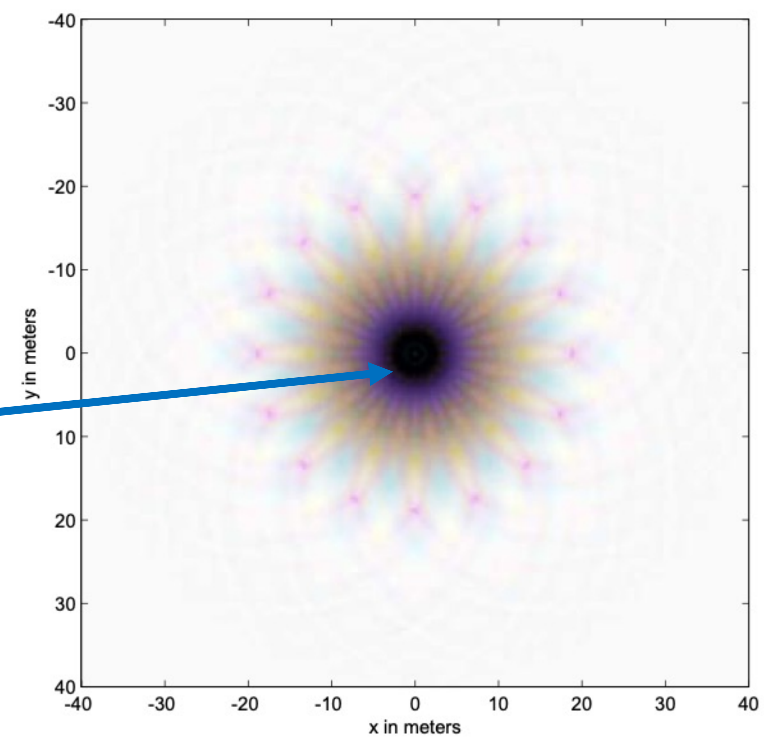

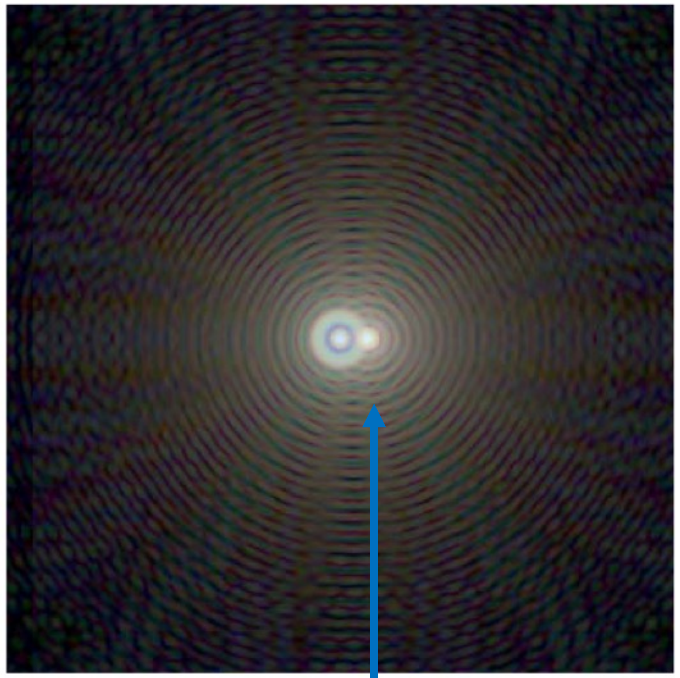

Suppression

Contrast

Shadow

The shadow is designed to be larger than the telescope pupil to allow for lateral motion. For the HWO concept, we designed the shadow to be 10 m in diameter, for a +/- 2 m radial tolerance.

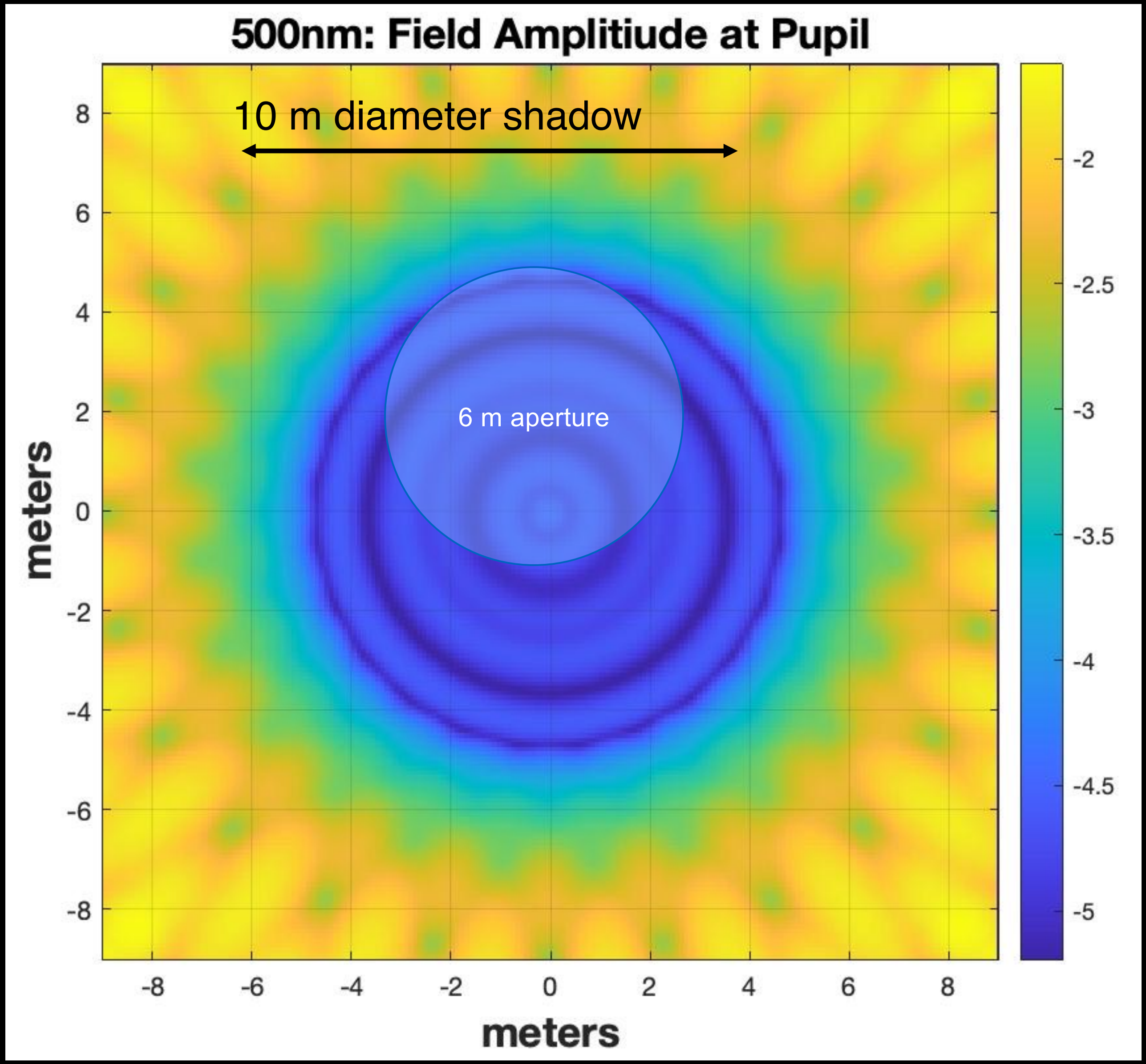

With a +/- 2 m radial tolerance, the sensing requirement is significantly relaxed compared to laboratory results, and the formation control bandwidth is ~ 600 s.

'Modern' History of Starshade Studies

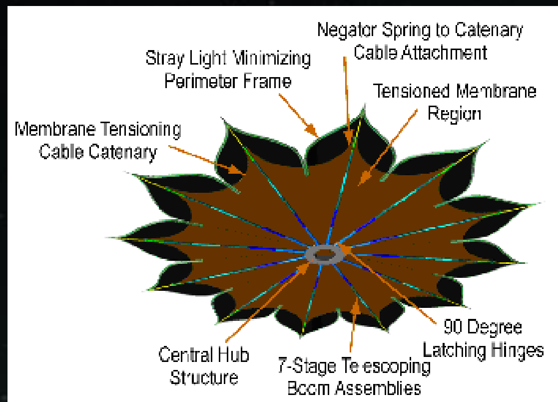

New Worlds Observatory, 50 m, Cash 2008

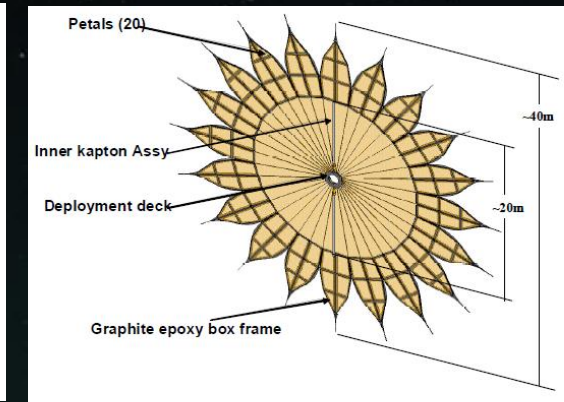

THEIA, 40 m, Kasdin 2009

Exo-S Dedicated, 2014

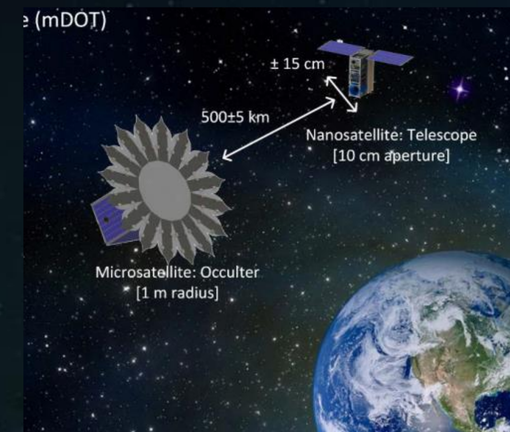

mDot, 3 mKoenig 2015

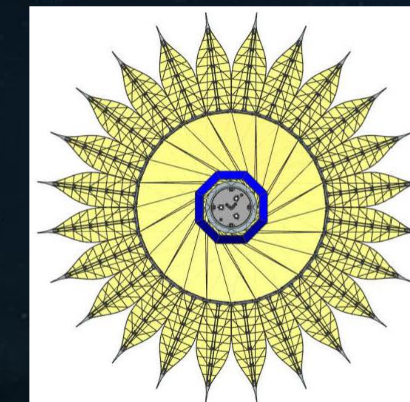

O3, 16 m, Lisman 2019

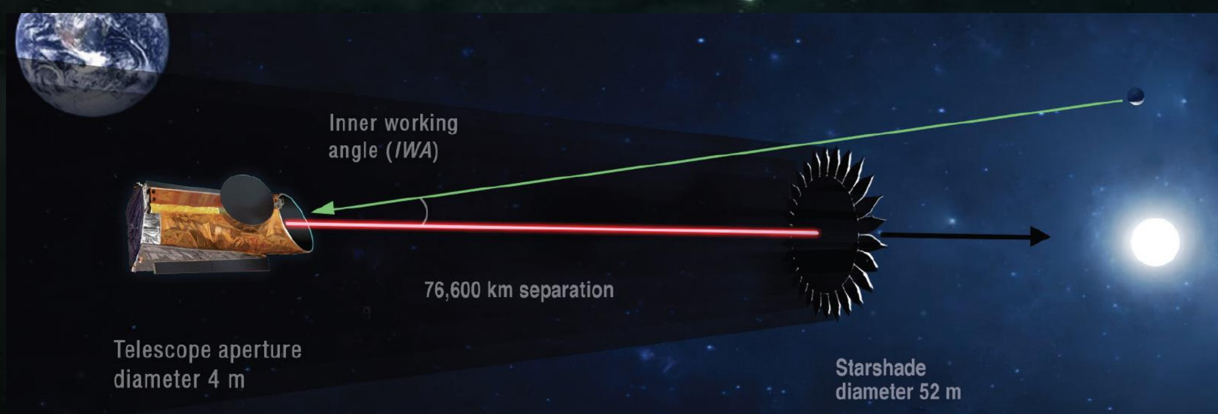

HabEx, 52 m, 2019

SRM, 26 m, Seager & Kasdin 2019

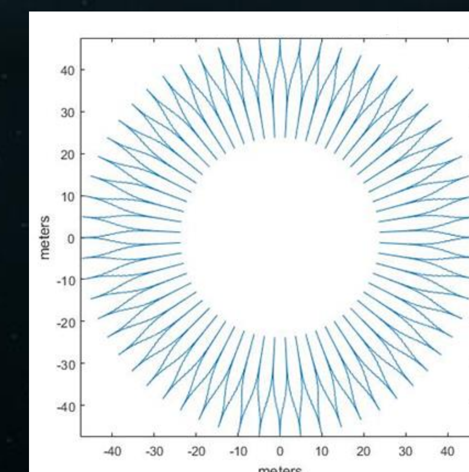

HOEE, 100 m
Mather 2020

- HWO concept parameters:
  - Tip width: 16 mm
  - Gap width: 2.1 mm
  - Petal length: 16 m
  - Disk Diameter: 28 m

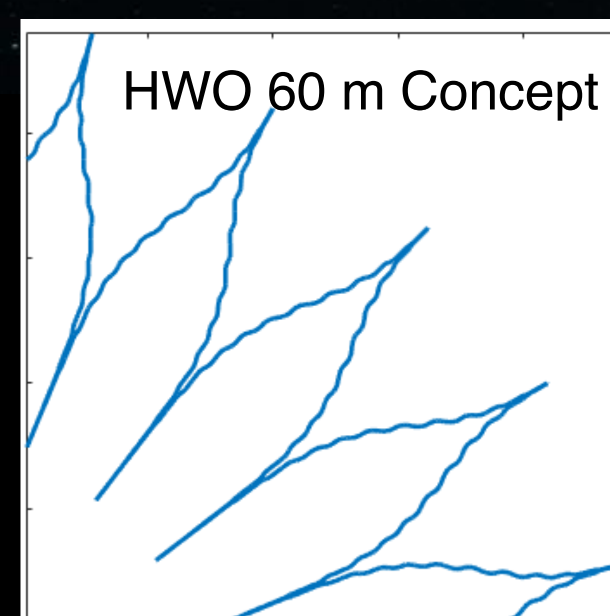

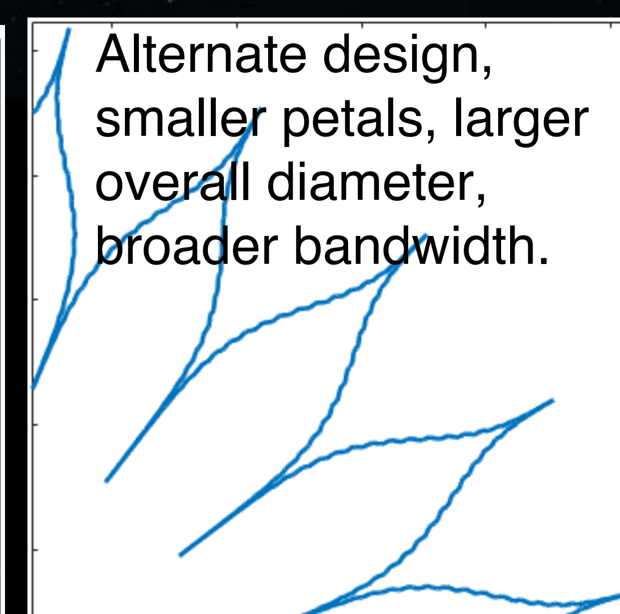

Simulated Solar System

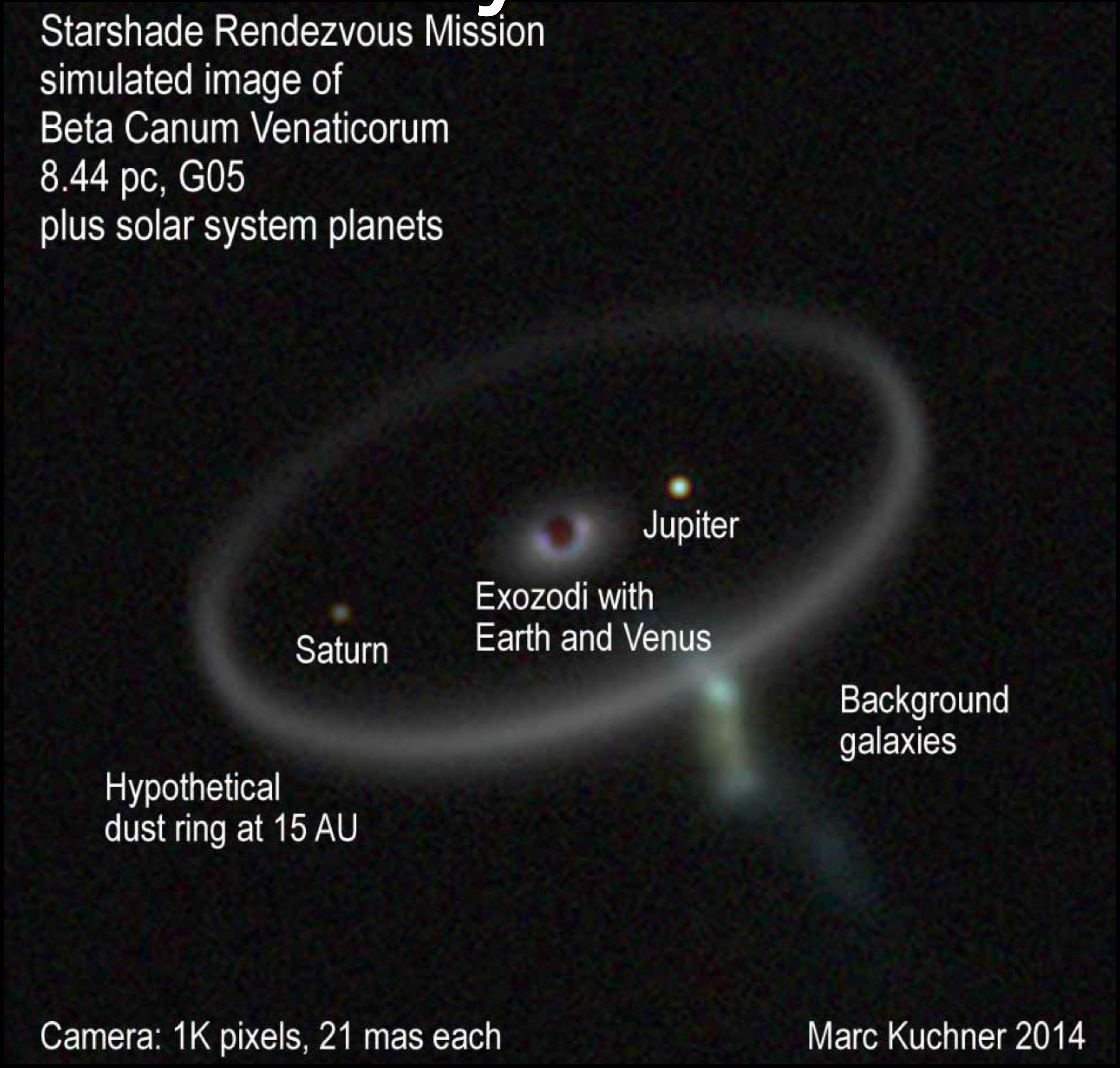

Size: Examples

Telescope	Tel. Diam. (m)	Bandpass (nm)	IWA (mas) Tip / 50%	Starshade Diam. (tip to tip, m)
HWO	6	500-1000	65 / 51	60
HWO (UV)	6	225-500	65 / 51	35
HabEx	4	300-1000	70 / 58	52
Roman Rendezvous	2.4	615-800	104 / 85	26

Starshade diameter scales more slowly than telescope diameter.
The HWO concept starshade has a diameter of 60 m and an $IWA_{0.5}$ of 51 mas.

The HWO $IWA_{0.5}$ is just 1.48 λ/D.

Metrics (same as coronagraph)

- Contrast: The ratio of the peak of the stellar point spread function to the halo at the planet location.
- Inner Working Angle: The smallest angle on the sky at which the needed contrast is achieved and the planet is reduced by no more than 50% relative to other angles.
- Throughput: The ratio of the light in the planet PSF to the nominal telescope PSF after high-contrast is achieved.
- Bandwidth: The wavelengths at which high contrast is achieved.
- Sensitivity: The degree to which contrast is degraded in the presence of aberrations.

Contrast

Starshade designs with reasonable engineering constraints will perform better than 1e-10. Here are the diffraction patterns for the HWO 60 m starshade (the as designed shape, no perturbations).

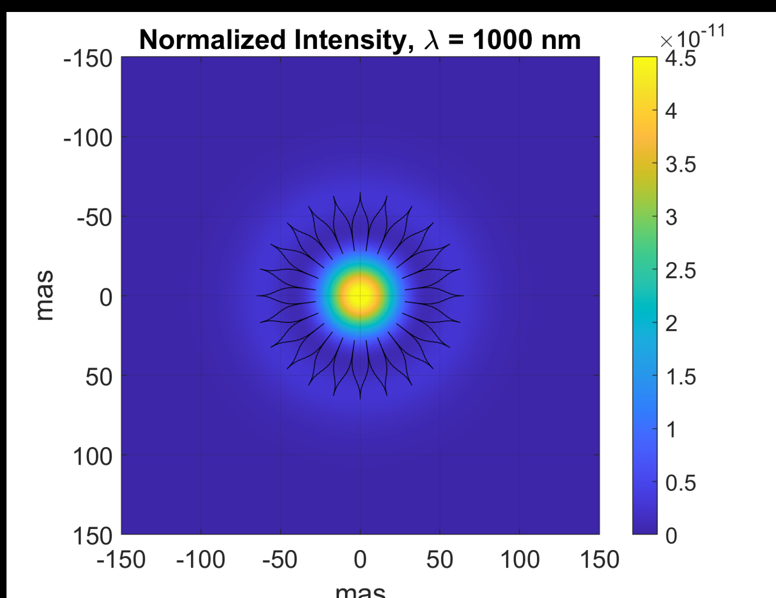

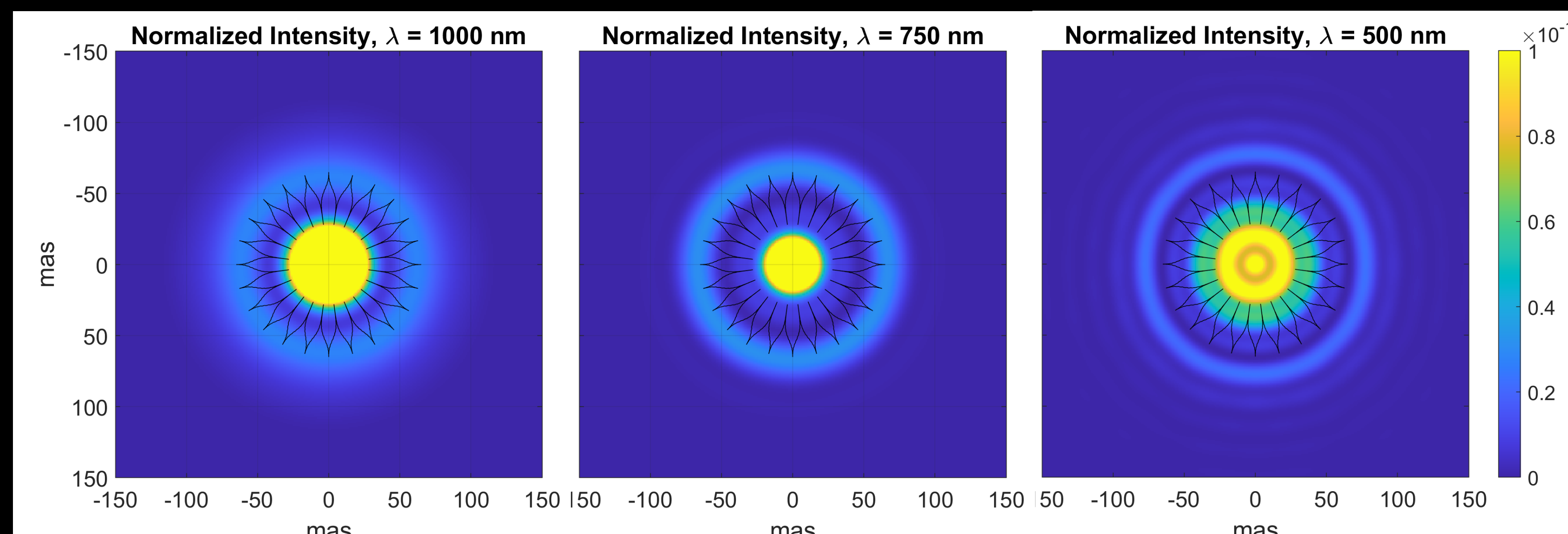

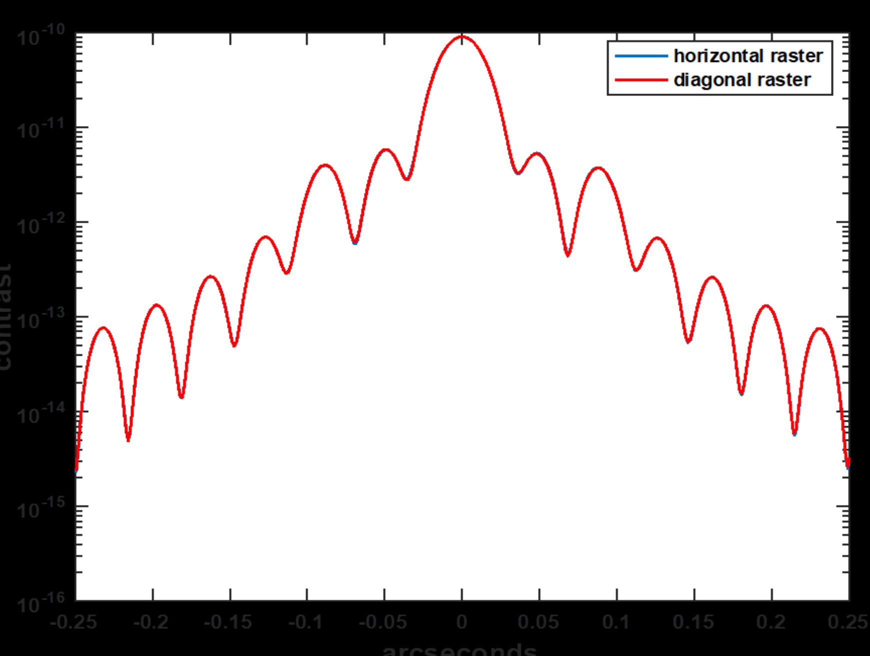

The design contrast at the IWA is ~ 5e-12. In practice, with lab-proven tolerancing, the instrument contrast at the IWA will be ~4e-11.

Contrast improves with working angle, ringing down to nearly zero at 150 mas. There is no outer working angle limitation.

Contrast: Solar Glint Lobes

The brightest contributors to instrument background near the IWA are the two solar glint lobes resulting from the Sun illuminating the edges of the starshade. Here we simulate imaging of a G4V V=5.65 star.

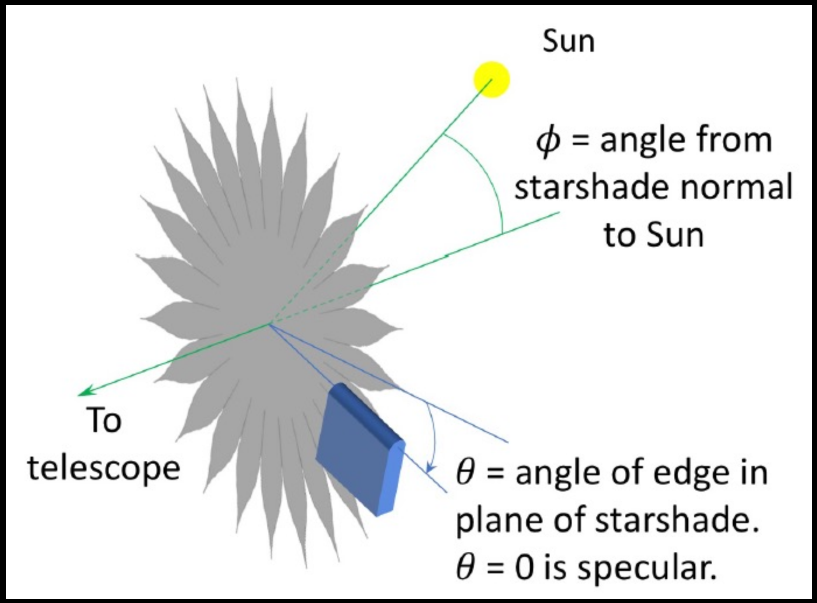

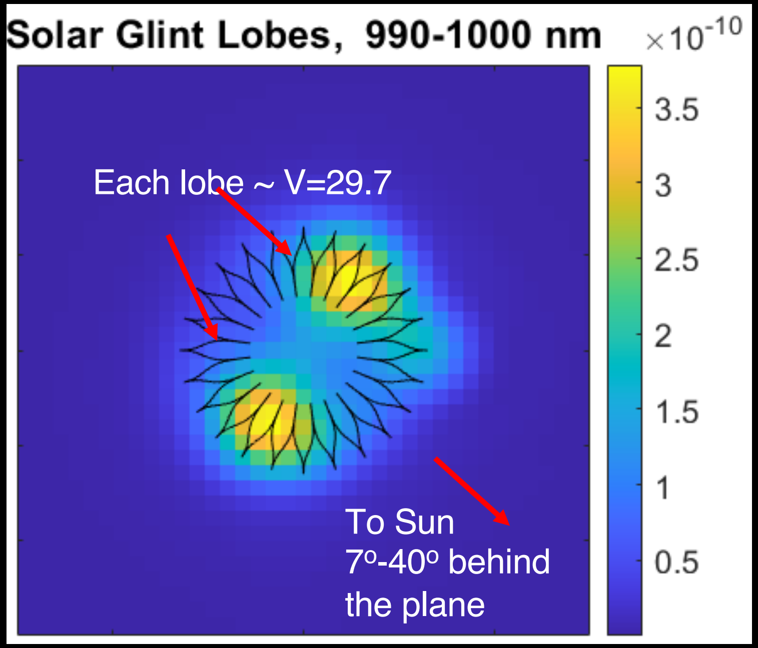

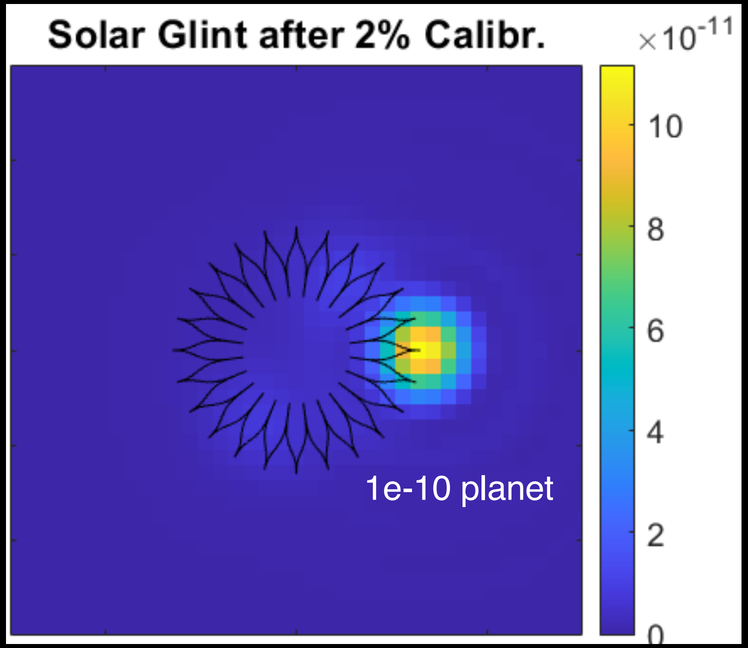

The brightness of solar glint lobes is mitigated by employing sharp, anti-reflection coated edges. Highly accurate calibration is performed during initial on-orbit checkout by moving the starshade closer to the telescope.

Solar glint lobes will have a visual magnitude of ~ 30 averaged over the IWA.

Throughput

Starshade throughput approximately follows the geometric opening of the petals (shown here). Instrument throughput is high because the cameras and spectrometers are relatively simple.

For exoplanet characterization, overall throughput is high due to a combination of:

- High starshade throughput
- High camera throughput
- Large instantaneous bandwidth
- Small calibration overhead

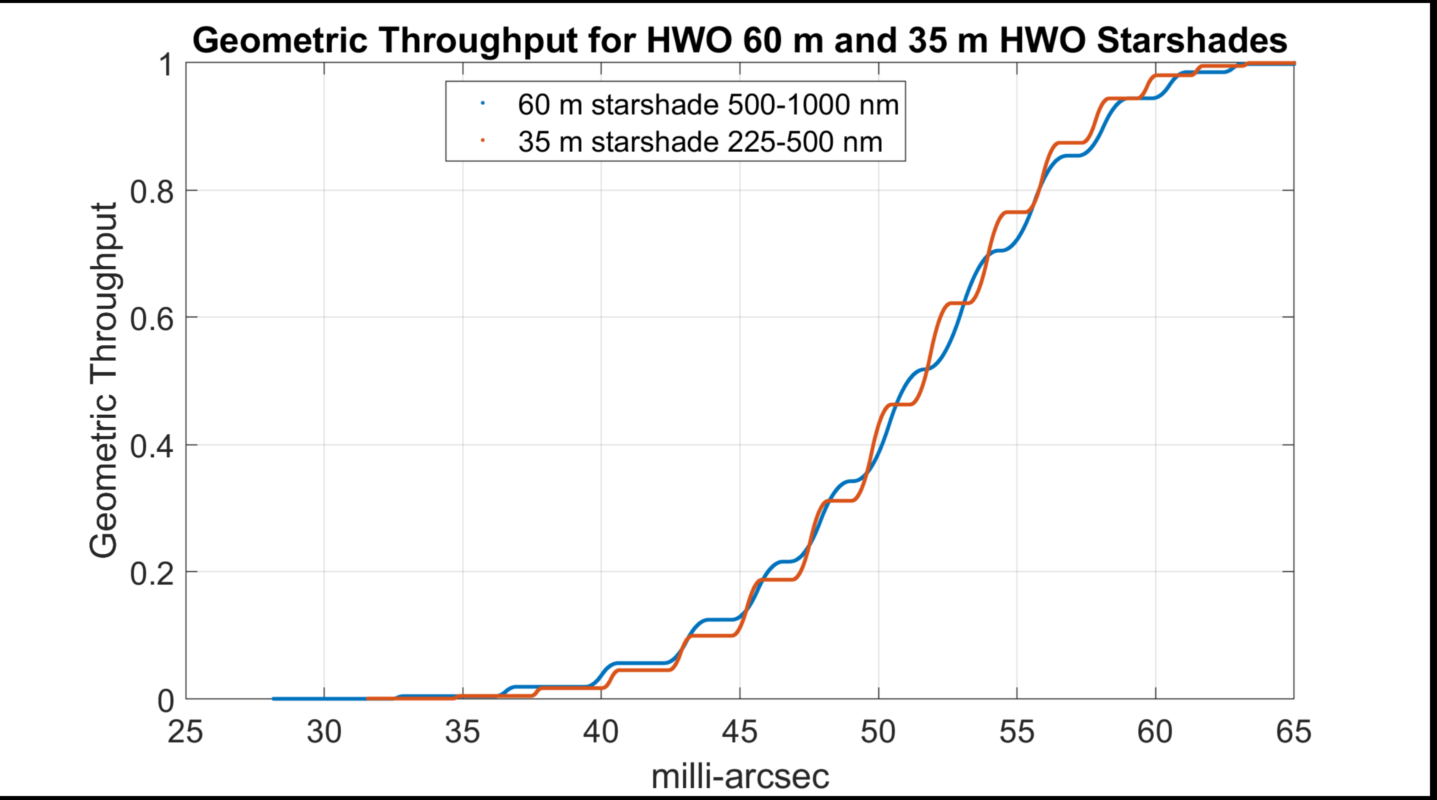

Bandpass and IWA

The same starshade can be used at ANY maximum wavelength. The IWA scales with wavelength.

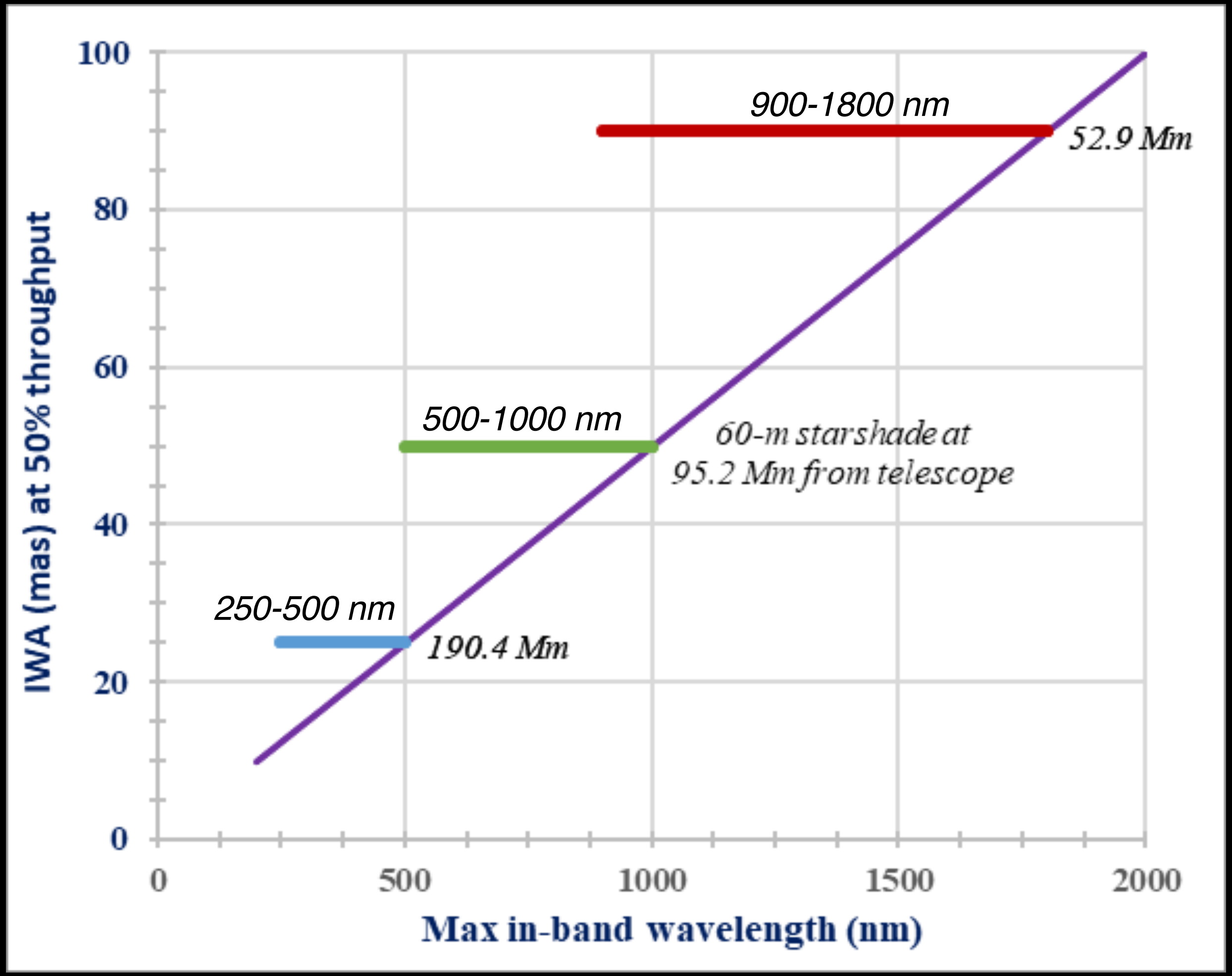

Bandpass (nm)	IWA (mas) Tip / 50%	Distance (Mm)
250-500	32.5 / 43	190.4
500-1000	65 / 51	95.2
900-1800	117 / 92	47.6

Bandpass (nm)	IWA (mas) Tip / 50%	Distance (Mm)
225-500	65 / 51	55.5
338-750	97.5 / 76	37.0
450-1000	130 / 102	27.8

For the 60 m, the $IWA_{0.5}$ is at 1.48 λ/D.

Bandwidth

A semi-infinite bandpass ($\lambda < \lambda_{max}$) is achievable but requires a starshade with long, narrow tips.
A finite bandpass is desirable because the bright light leaking on either side of the suppression band can be used for formation flying.

We use HabEx as an example. HWO will be similar.

When positioned for the visible band (green line), the red box 1.6-1.8 um provides the formation flying signal.

When positioned for the IR band, the blue box 0.3-0.5 um provides the formation flying signal.

The formation flying alignment signal is the leaked Poisson spot from the star.

Example out-of-band guiding signal from HabEx report.

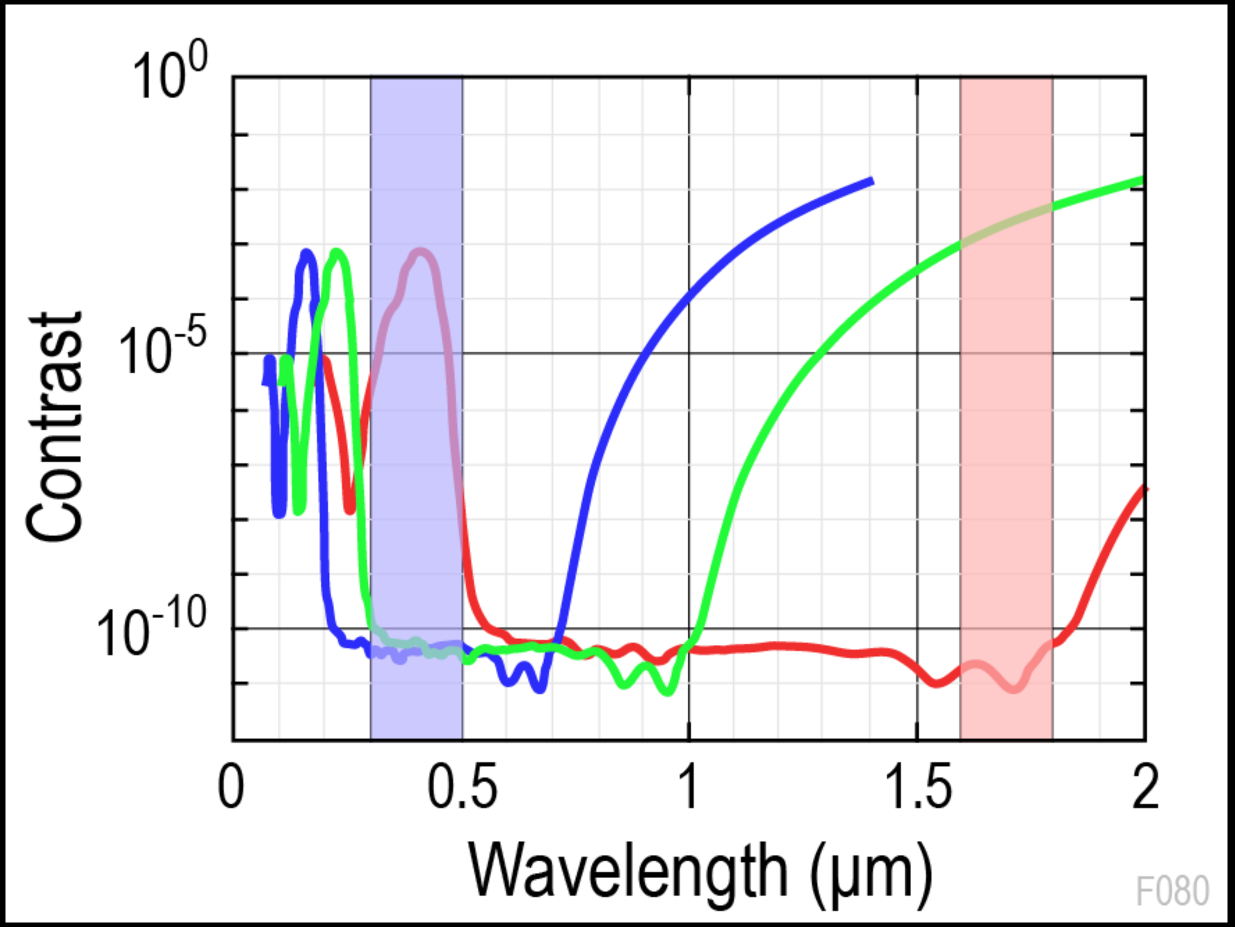

Summary of Key Advantages

Starshades remove the starlight before it can scatter in the telescope.

Parameter	Starshade	Demonstrated
IWA	>1.2 λ/D	1.8 λ/D
Bandwidth	> 100%	12.5%
Contrast	< 1e-10	1.15e-10 at IWA
Throughput	100%	90%
Telescope stability, shape, segmentation	Works equally well with any aperture shape, segmented or monolith, on- or off-axis. Does not drive stability.	Circular aperture

Making it Work

- Mechanical Design and deployment
- Error budgeting
- Manufacturing tolerances and stability
- Optical model verification

Generation 2 Perimeter Truss Design

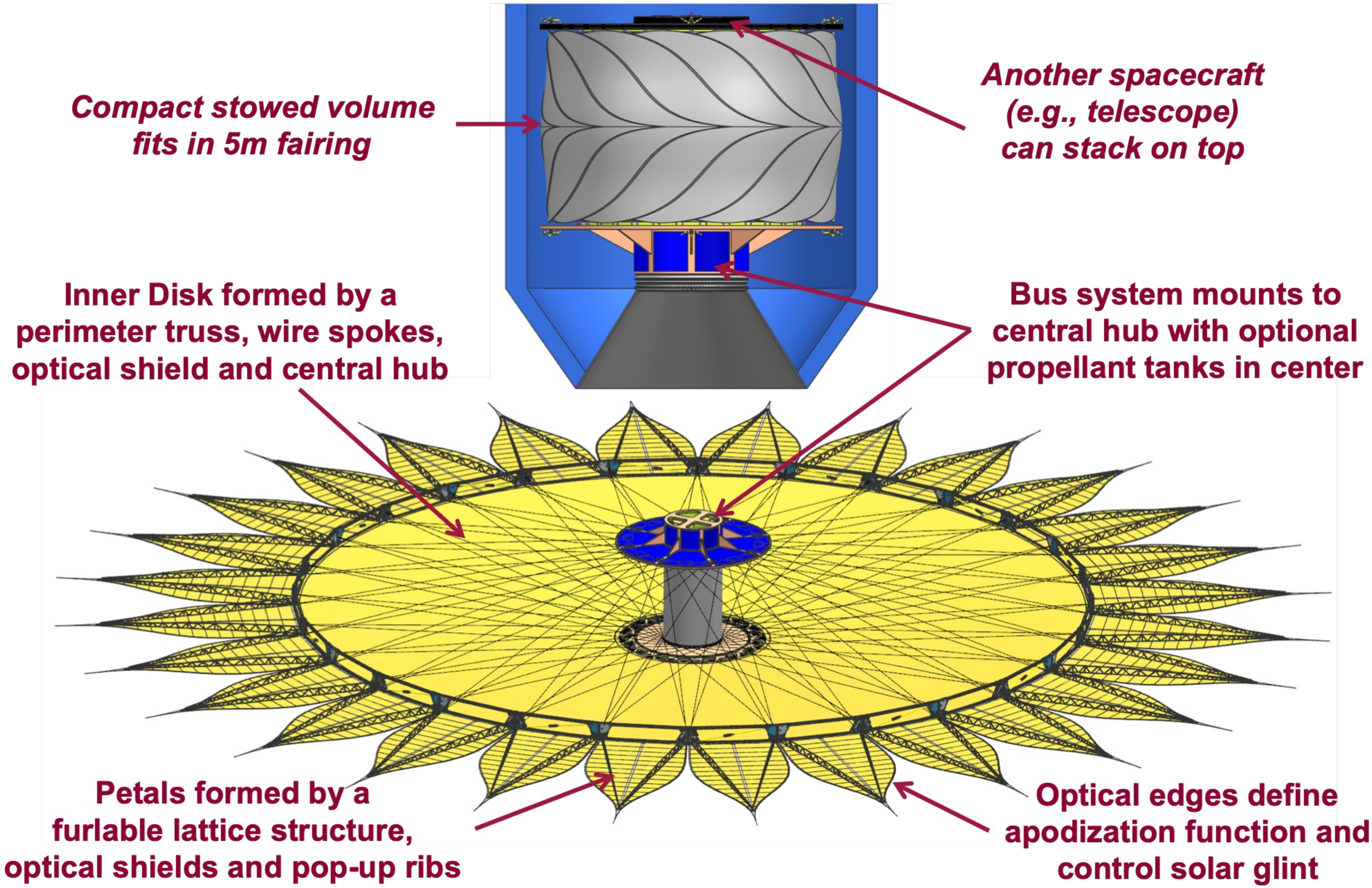

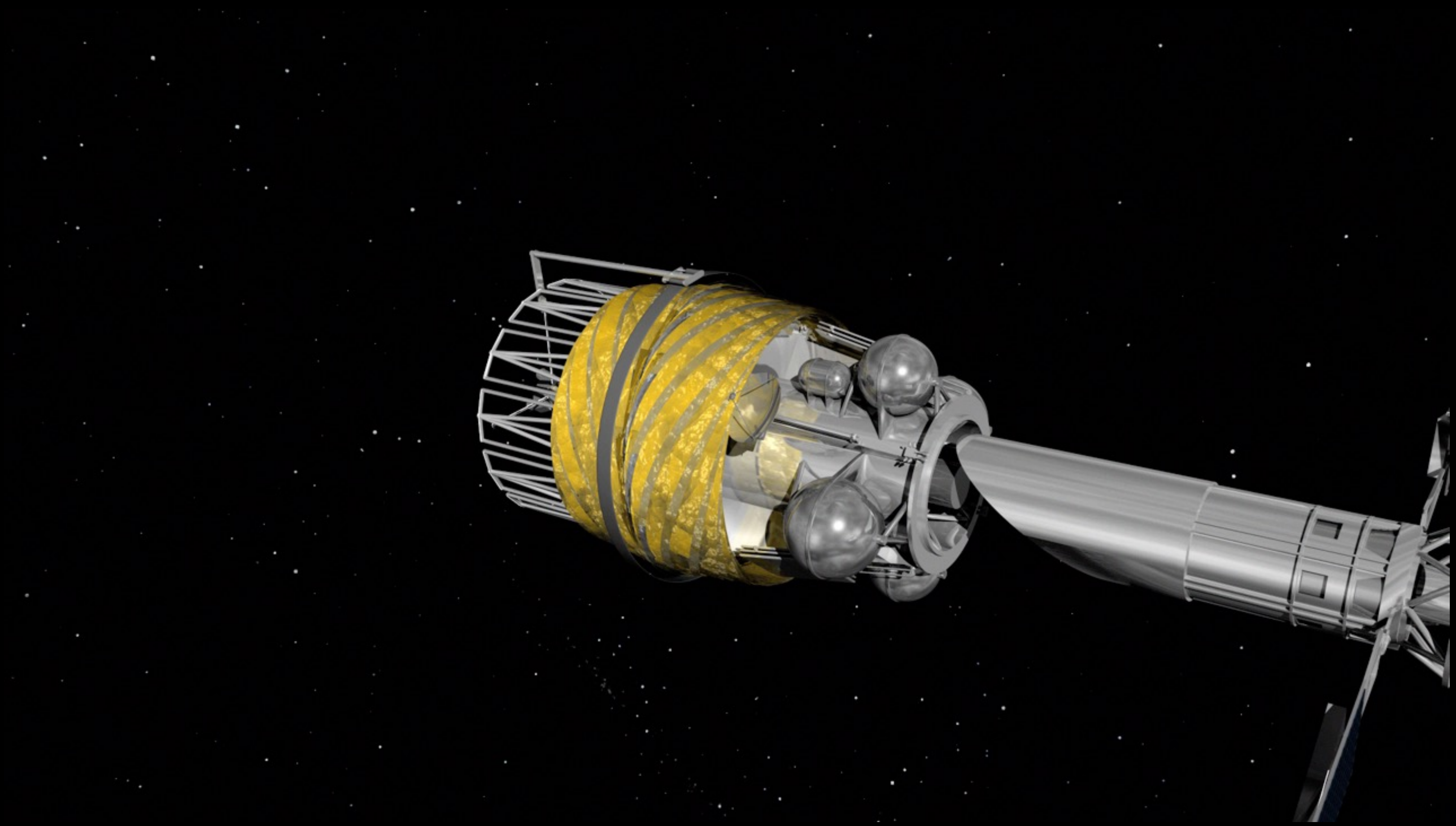

Gen 2 Deployment (no metrology)

Error Budget & Requirements

Employ a detailed error analysis examining all perturbations to set an error budget and requirements on manufacture and deployment.

Sensitivty – Error Budget Tree

Systematic Noises Sources

Photometric Noises Sources

Background objects, solar glint, earthshine, moonshine, milky way and other bright bodies

Propulsion plume, telescope scatter

All systematics + detector read noise, dark current, cosmic rays

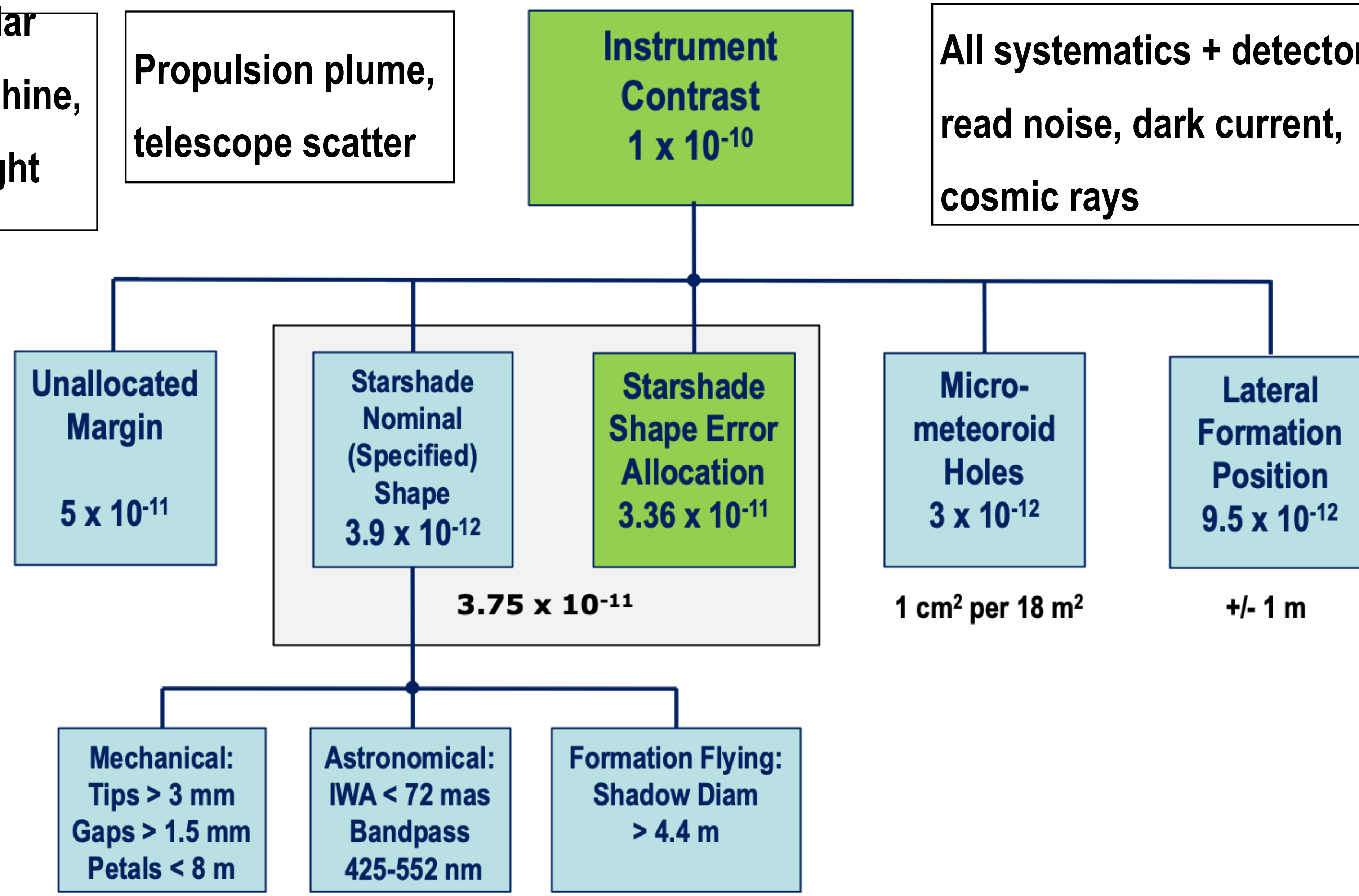

Shape Allocation breakdown

Char. Feature		CBE 3 sig	Cont.	Max Exp.	CBE Cont	Max Exp Cont
Petal Width (um)	Bias	20.00	0.25	2.50E+01	5.68E-13	8.88E-13
Edge Segment x and y position (um)	Random	20.00	0.25	2.50E+01	5.54E-13	8.66E-13
Edge Segment x and y position (um)	Bias	10.00	0.25	1.25E+01	4.97E-13	7.76E-13
Edge Segment clocking (urad)	Random	33.33	0.25	4.17E+01	4.27E-13	6.67E-13
Edge Segment shape (sinusoidals) (um)	Bias	13.00	0.50	1.95E+01	3.54E-13	7.96E-13
Petal Interface radial position (mm)	Random	0.17	0.25	0.21	1.85E-13	2.88E-13
Tip segment width (um)	Bias	13.00	0.50	1.95E+01	1.22E-13	2.75E-13
Petal higher order (sinusoids) (um)	Bias	1.00	1.00	2.00E+00	1.13E-13	4.52E-13
Edge Segment shape (sinusoidals) (um)	Random	13.00	0.50	1.95E+01	1.02E-13	2.29E-13
Tip segment shape (sinusoids) (um)	Bias	13.00	0.50	1.95E+01	7.62E-14	1.71E-13
Tip segment width (um)	Random	13.00	0.50	1.95E+01	6.76E-14	1.52E-13
Edge Segment Shape residual (f> 3 cycles/segment)	Bias	13.00	0.50	1.95E+01	5.41E-14	1.22E-13
Petal Interface radial position (mm)	Bias	0.04	0.25	0.04	4.82E-14	7.53E-14
Petal Interface clocking angle (urad)	Random	100.00	0.25	0.00	4.39E-14	6.85E-14
Tip segment shape (sinusoids) (um)	Random	13.00	0.50	1.95E+01	4.23E-14	9.51E-14
Edge Segment clocking (urad)	Bias	5.00	0.25	6.25E+00	2.97E-14	4.63E-14
Petal Interface elliptical mode (mm)	Bias	0.10	0.50	0.15	2.34E-14	5.26E-14
Petal Interface tangential position (mm)	Random	0.03	0.25	0.03	6.30E-15	9.84E-15
Tip segment x and y position (um)	Random	20.00	0.25	2.50E+01	2.02E-15	3.16E-15
Tip segment x and y position (um)	Bias	10.00	0.25	1.25E+01	9.12E-16	1.42E-15
Petal Interface higher order polygon modes (mm)	Bias	0.10	0.50	0.15	8.66E-16	1.95E-15
Petal 1-cycle in-plane shape error (width preserving) (mm)	Random	0.03	0.50	3.75E-02	1.77E-16	3.97E-16
Quadratic bending (cantilever beam bending) (mm)	Random	0.05	0.50	7.50E-02	4.31E-18	9.71E-18
Tip segment clocking (urad)	Random	33.33	0.25	4.17E+01	3.85E-18	6.02E-18
Quadratic bending (cantilever beam bending) (mm)	Bias	0.05	0.50	7.50E-02	3.58E-22	8.06E-22
Tip segment clocking (urad)	Bias	5.00	0.25	6.25E+00	2.06E-23	3.22E-23
SUM					3.32E-12	6.04E-12

Experiment vs. Requirement

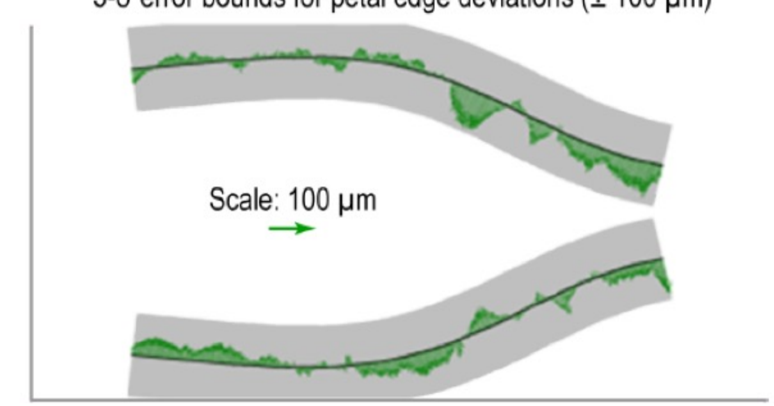

Figure 9.4-2. Measured petal shape error (green arrows) vs. 100 µm tolerance for 1×10^{-10} imaging (gray band) shows full compliance with the allocated tolerance.

Table 6.4-4. Comparison of TDEM results with Exo-S requirements.

Key Technology	Demonstration	Achieved Tolerance	Required Tolerance
Petal Segment Shape (Random)	TDEM-09	±45 µm	±68 µm
Petal Segment Position (Random)	TDEM-09	±45 µm	±45 µm
Radial Petal Position (Bias)	TDEM-10	±100 µm	±150 µm

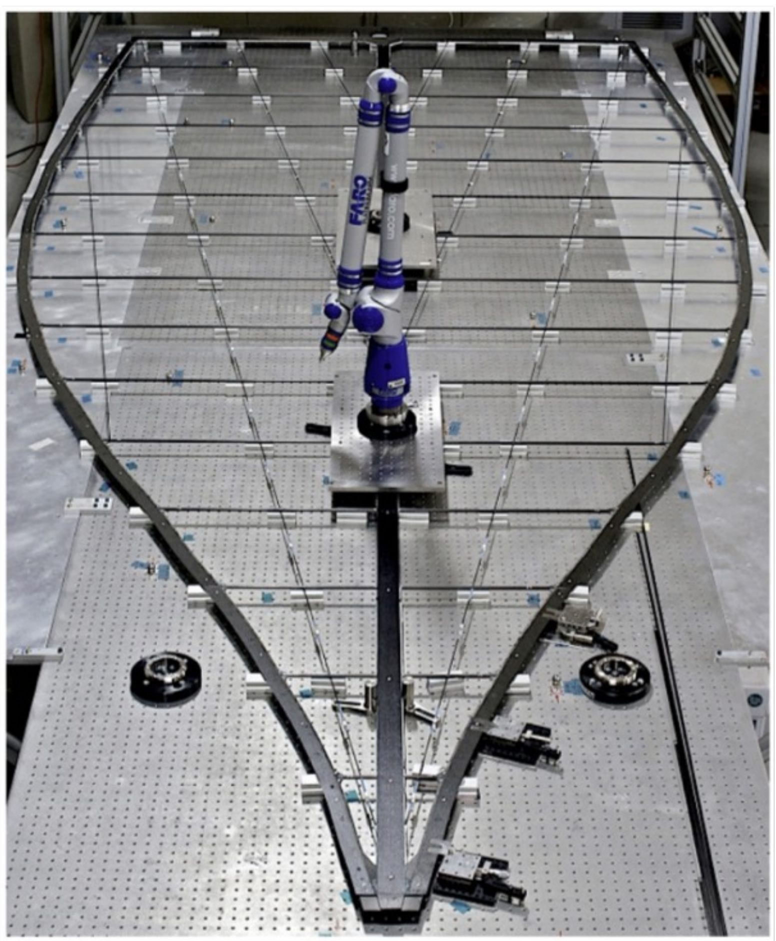

Kasdin TDEM-10 Final Report

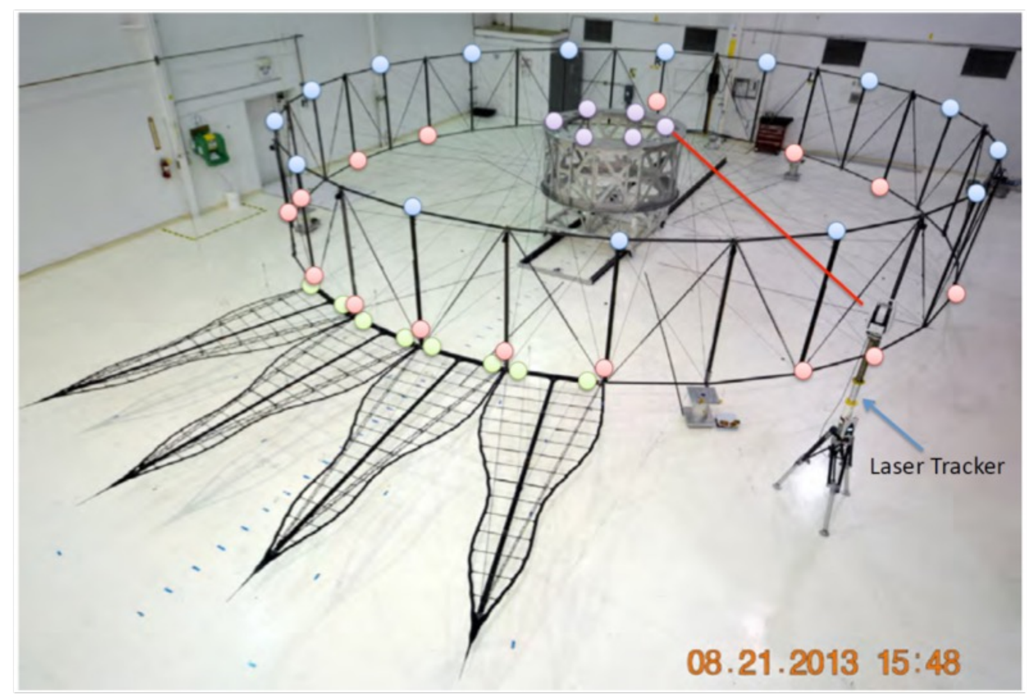

Kasdin TDEM-11 Final Report

Mean contrast at worst-case wavelength of 2.15×10^{-10}

Spinning the Starshade

- Benefits of spinning
  - Reduce local thermal shape variations
  - Circularize leakage from shape defects
    - Speckles smear into annuli, not to be confused with an exo planet.
    - Relaxes deformation requirements: driven by photometric leakage rather than systematic leakage.
    - But does not eliminate localized solar glint and formation flying scatter
  - No big reaction wheels
  - Robust fault tolerance
- Downside
  - Requires some additional fuel to rotate the angular momentum vector

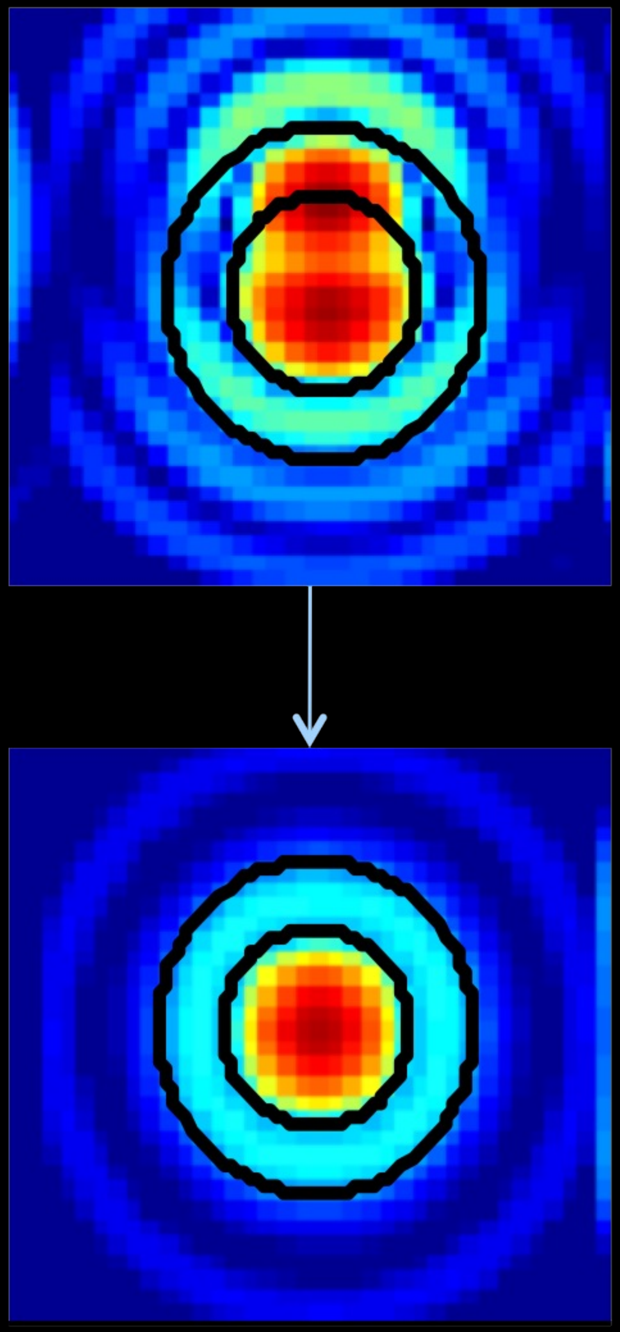

Shaklan, SPIE, 2011

Experimental Optical Verification

Verify the scalar optical modeling used for design and performance predictions is correct via subscale tests

Princeton Starshade Testbed

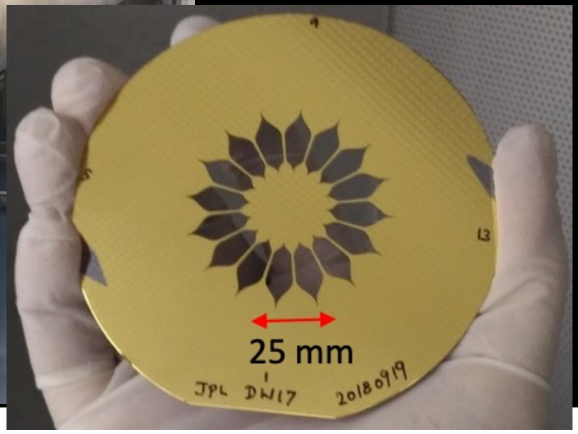

Conducted by Anthony Harness

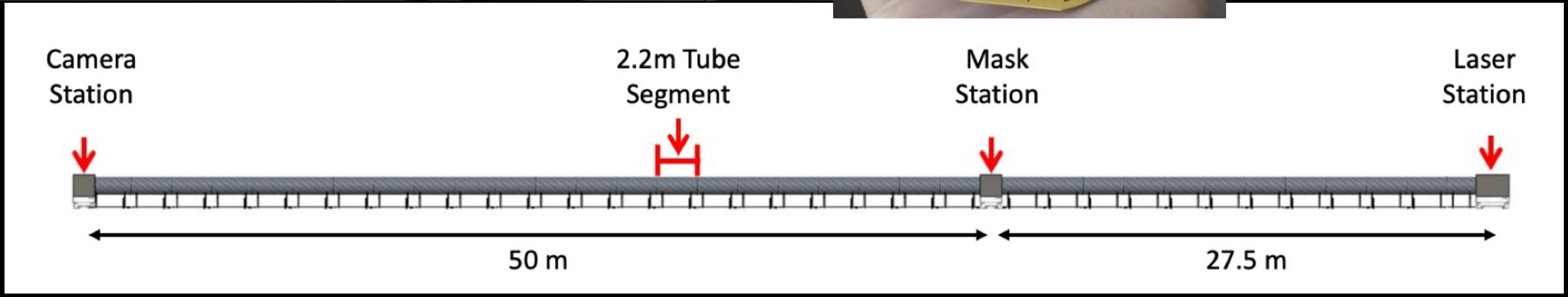

Laboratory Starshade Design at Flight Fresnel Number

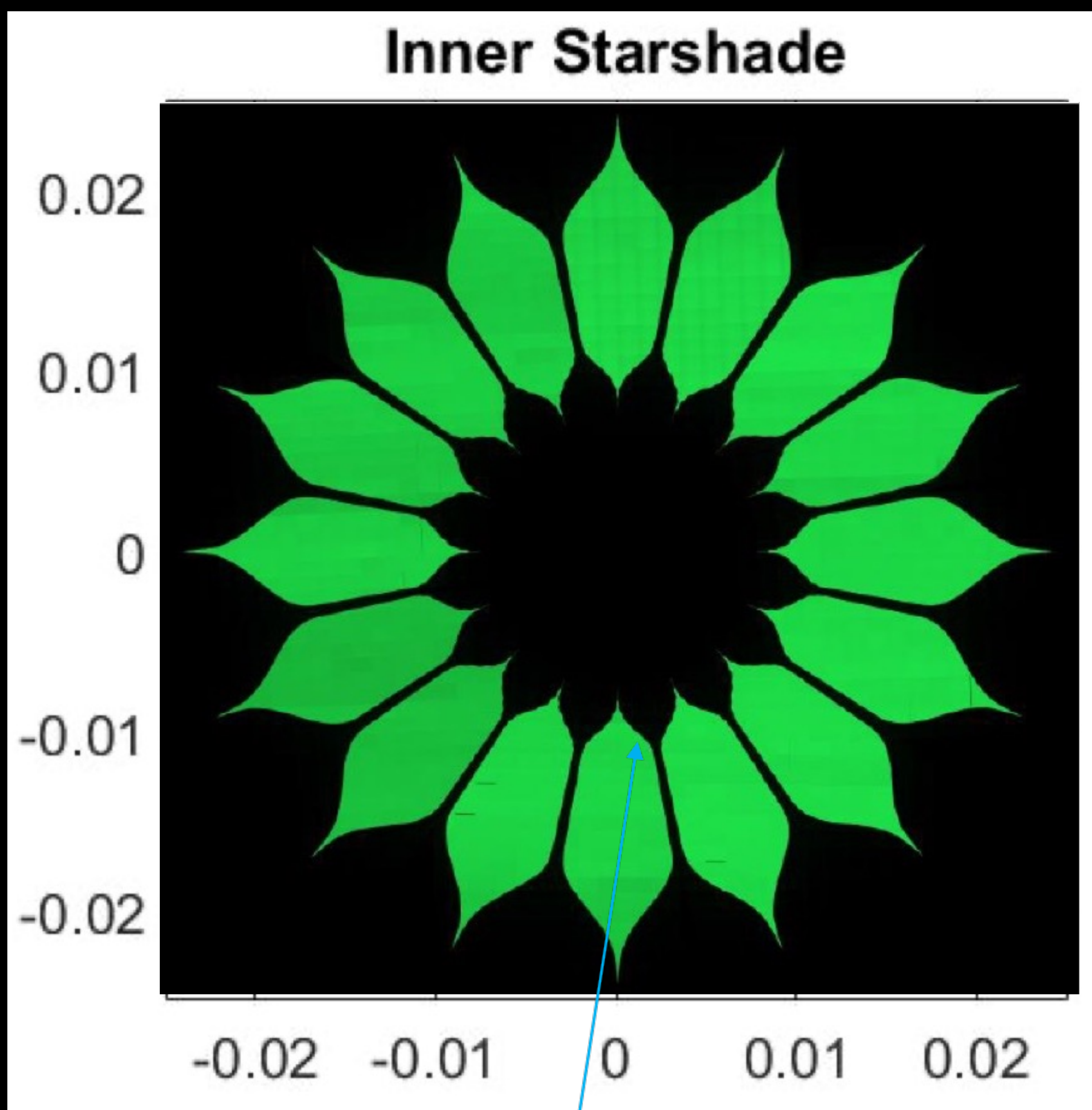

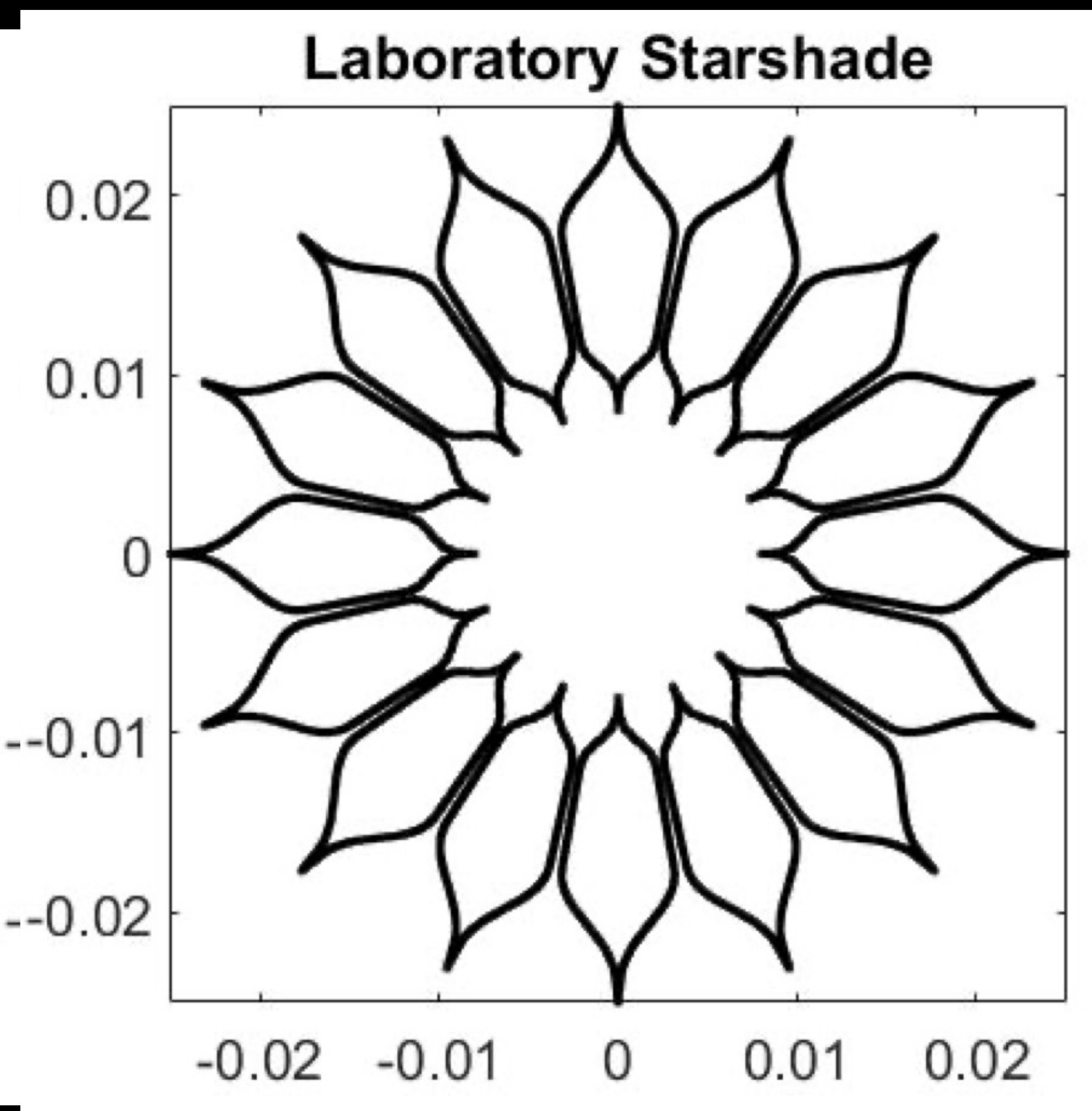

Inner Tips: 16.2 um wide, 500 um long
Outer Tips: 27 um wide.

Sample Lab Results

Single wavelength: 641 nm

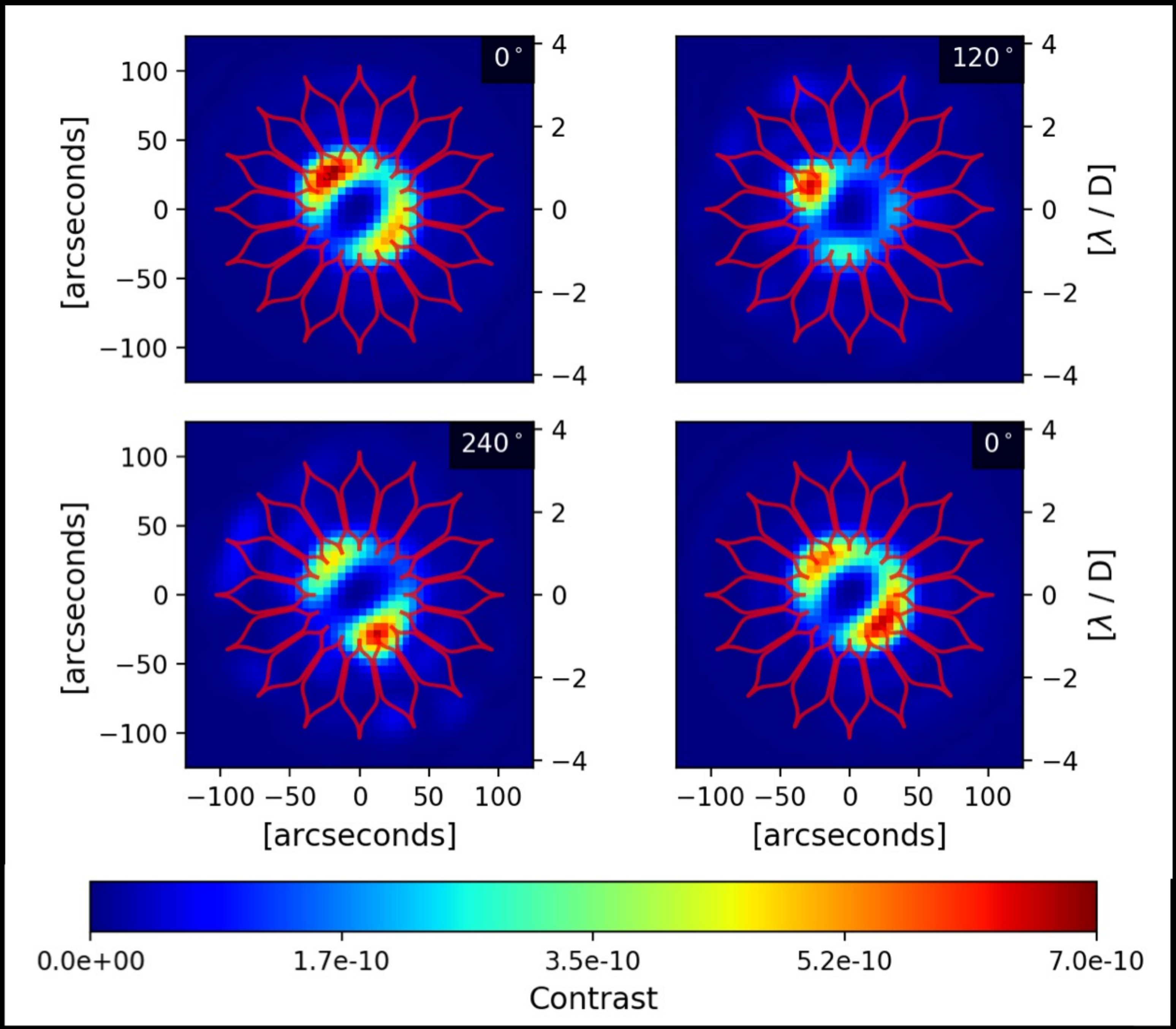

Bright lobes are due to interaction with the mask edge as light propagates through narrow valleys

"Thick Screen Effects"

Demonstrated ability to achieve 1e-10 contrast with lab starshade.

Operational Considerations

- Formation flying
- Viewing Constraints
- Solar diffraction and glint
- Slew time and DRMs

Retargeting and Stationkeeping

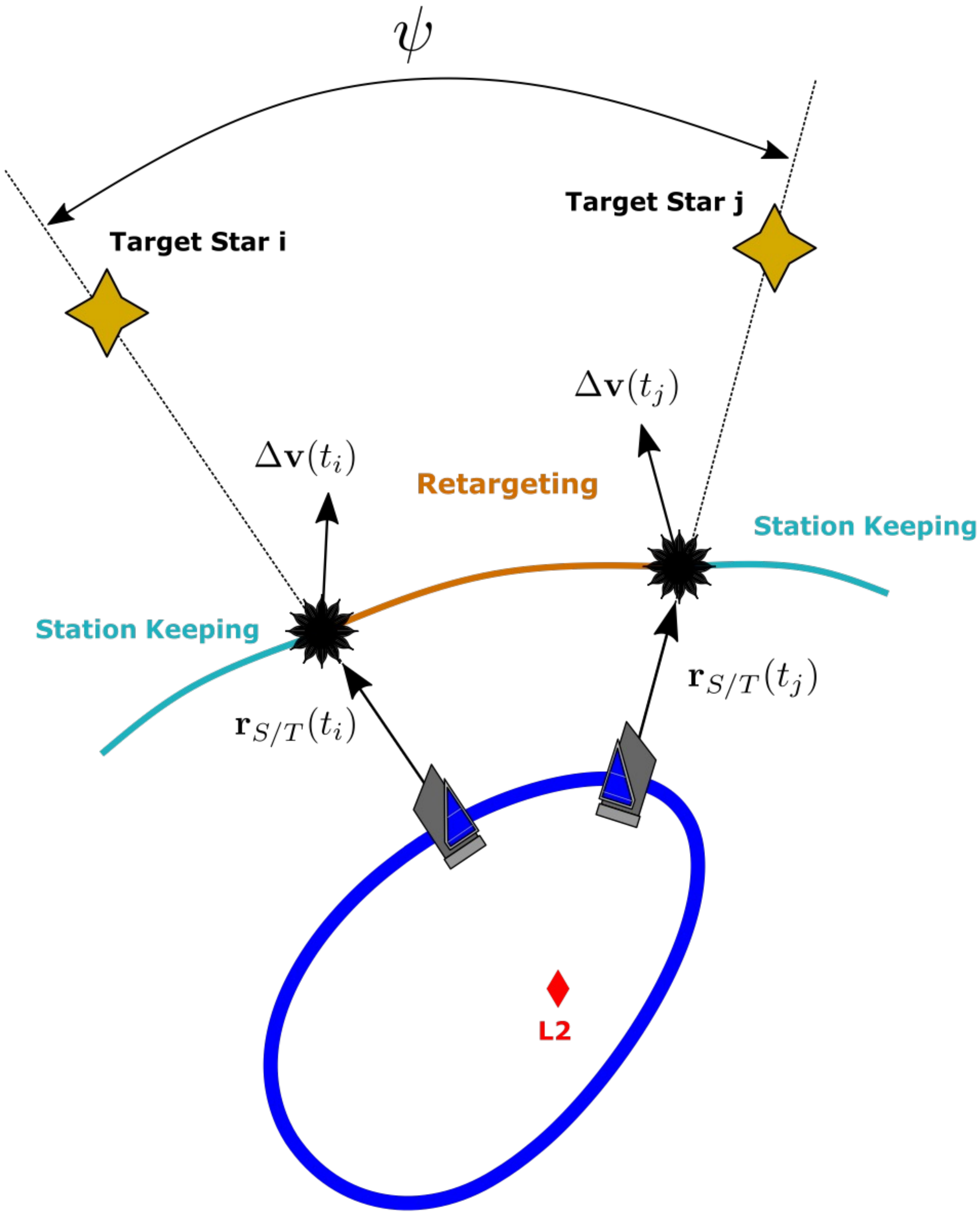

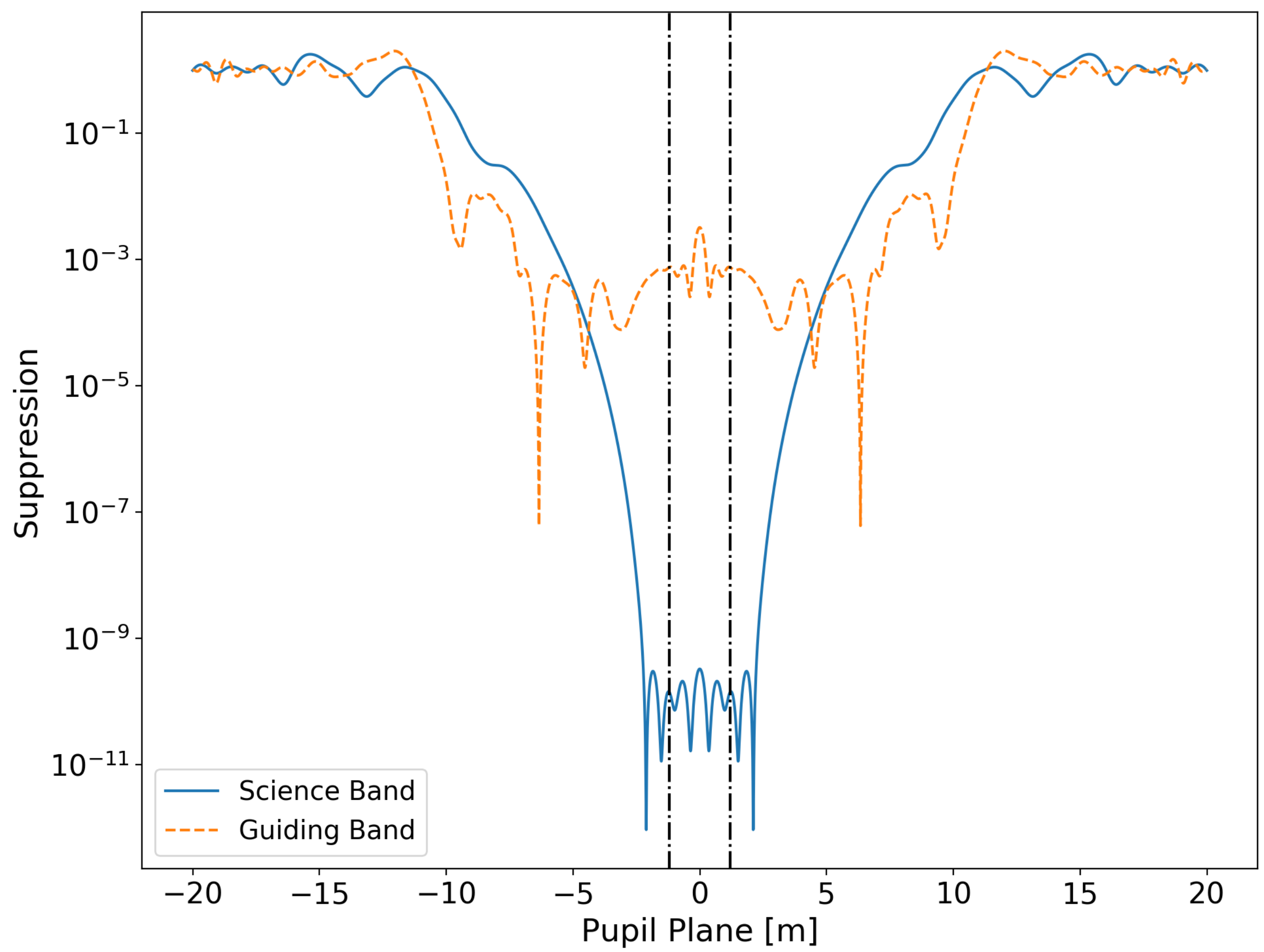

Soto, et al.

Control Loop

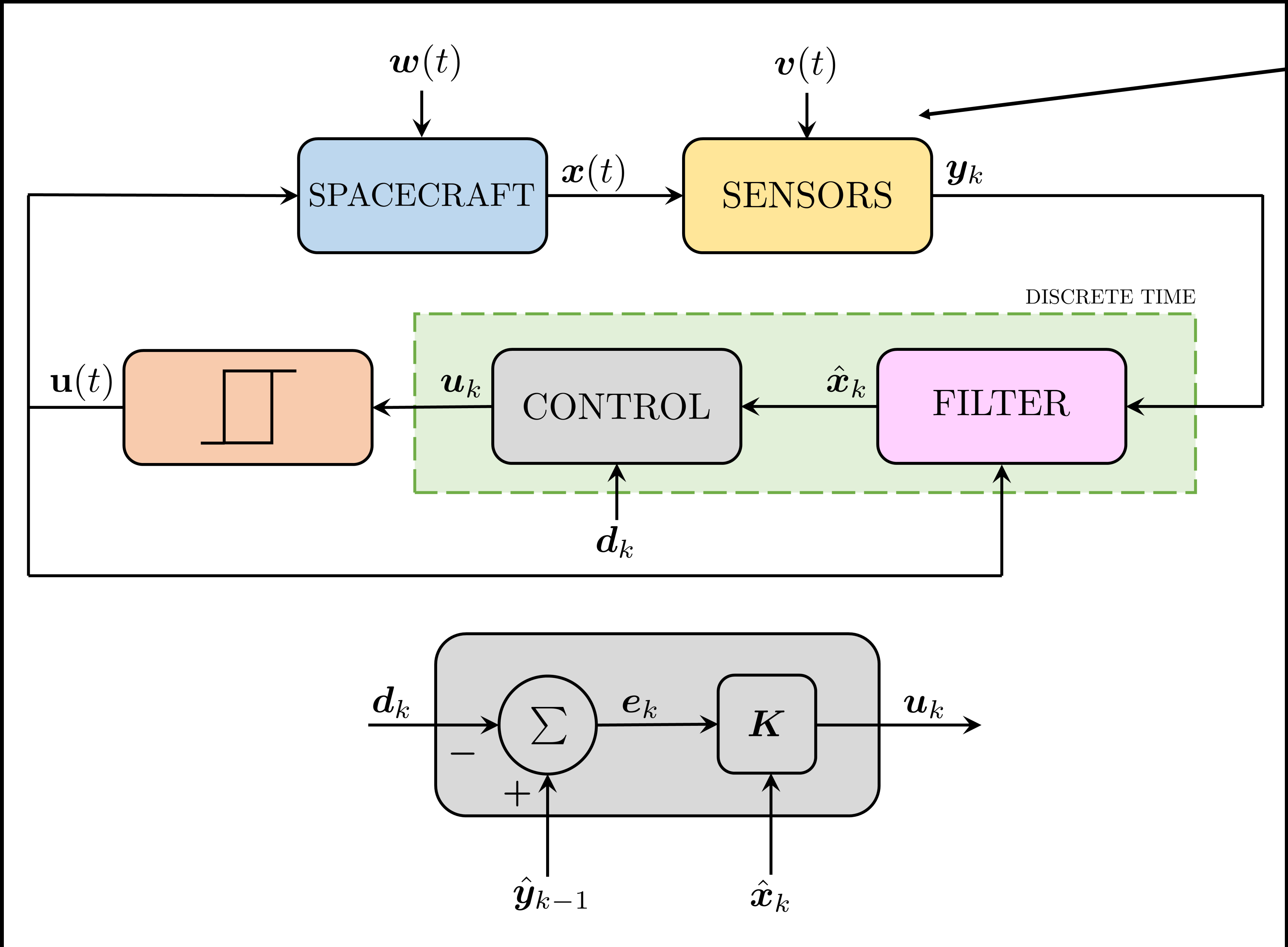

measure position by fitting pupil image

Linear Quadratic Regulator with Integral Control and Unscented Kalman Filtering

Hardware-in-the-loop Stationkeeping Test

Simulated Formation keeping with actual position measurements from Princeton testbed

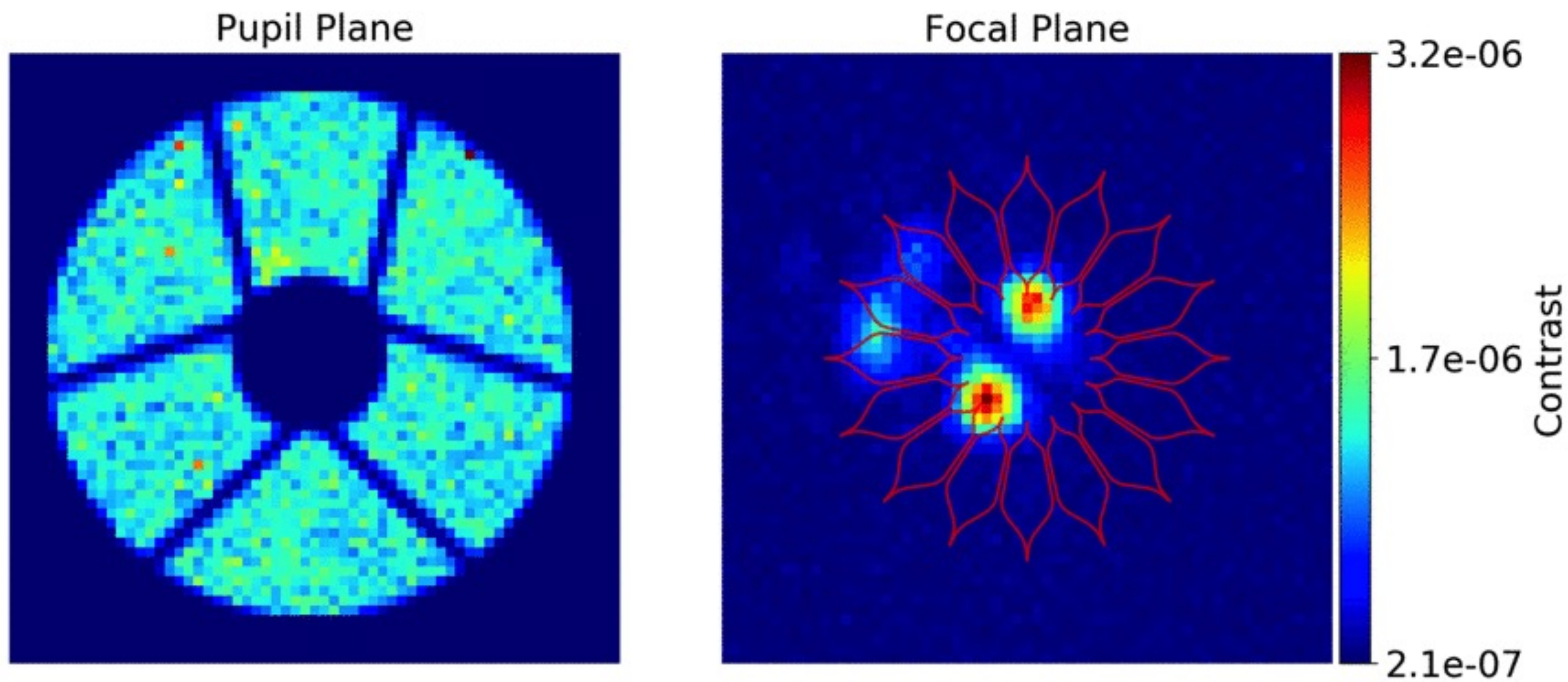

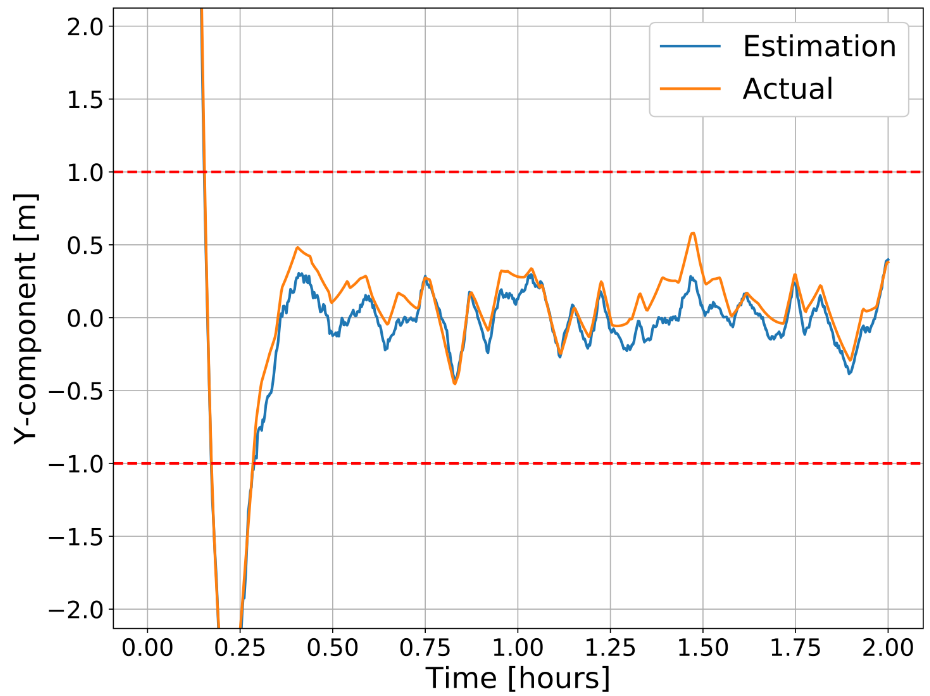

Viewing Constraints

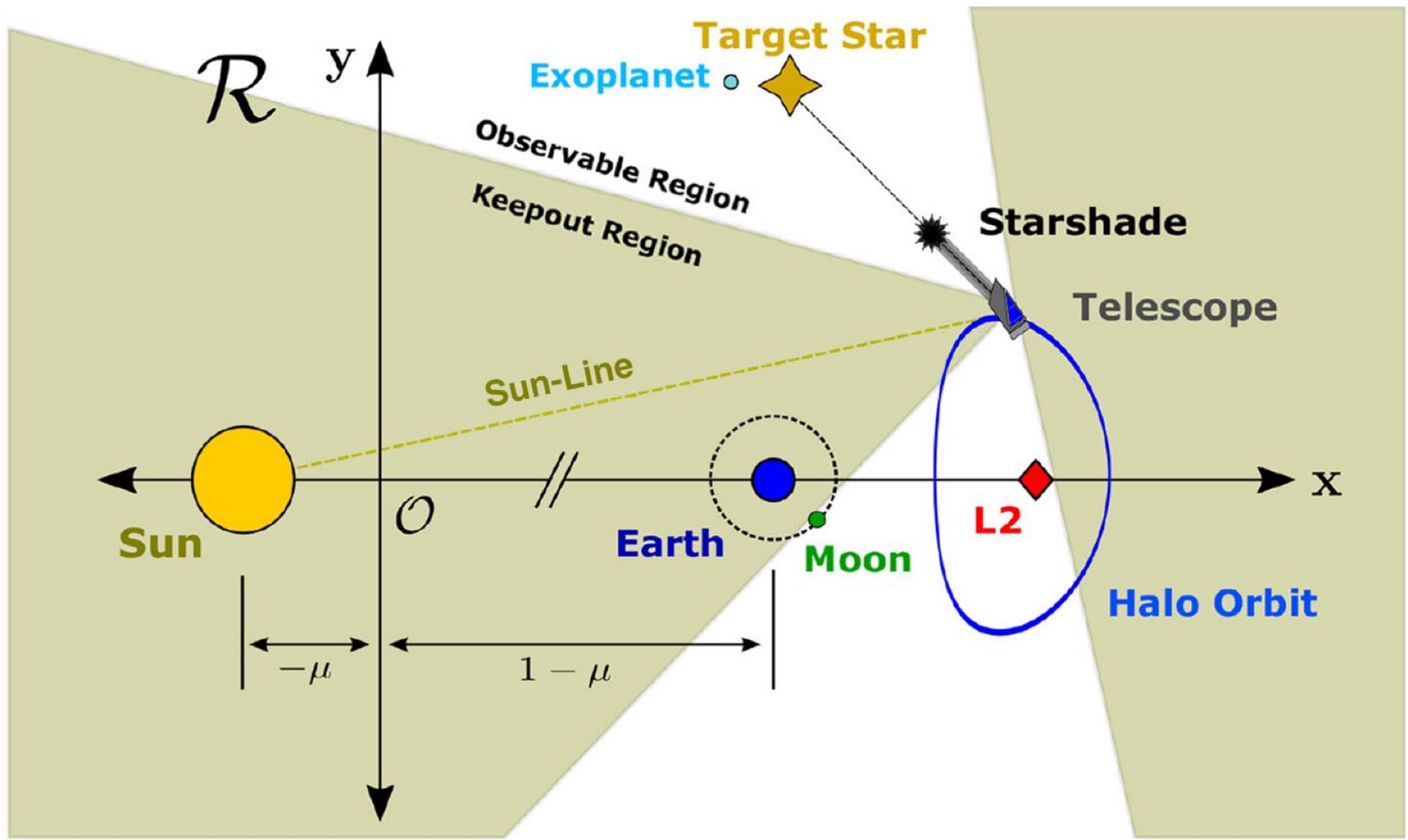

40 to 83 deg Field of Regard

Soto, et al.

Sample Target Availability

Starshade Rendezvous

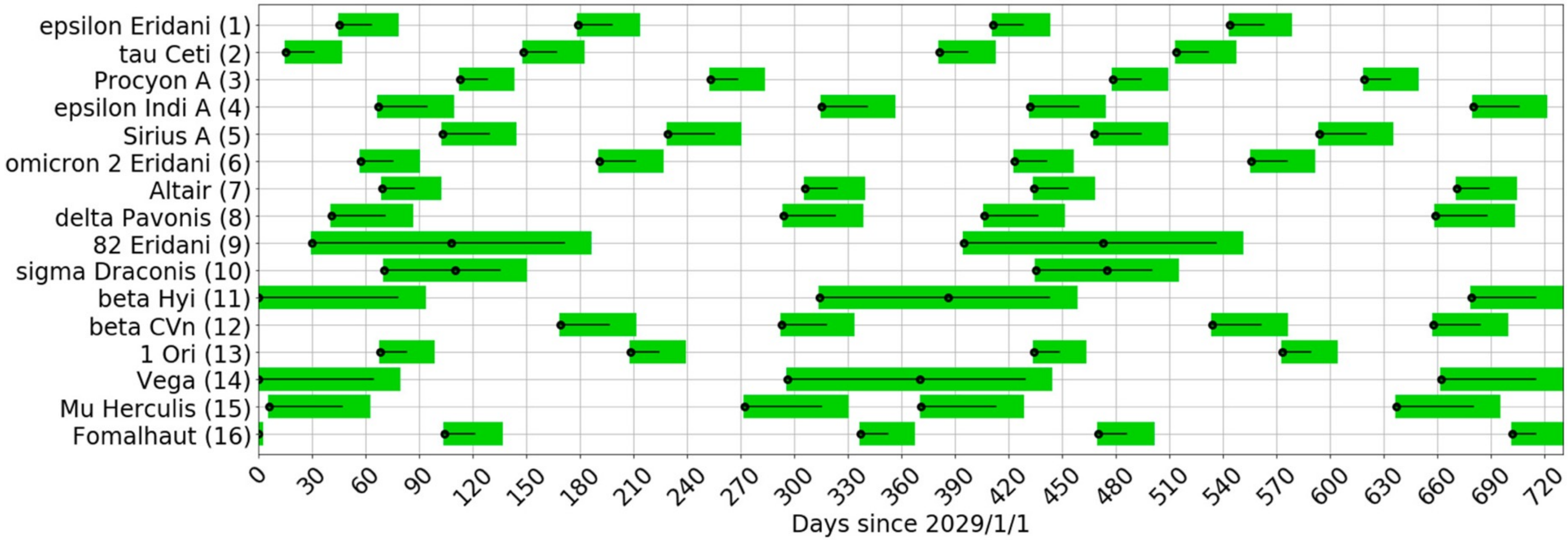

- Selected high completeness (>0.5) targets with no optical companions.
- Targets are distance range between 3 – 8 pc.
- Viewing windows determined by solar exclusion angles.
- Two ~30-day windows per target per year is typical.

Example DRM – Rendezvous

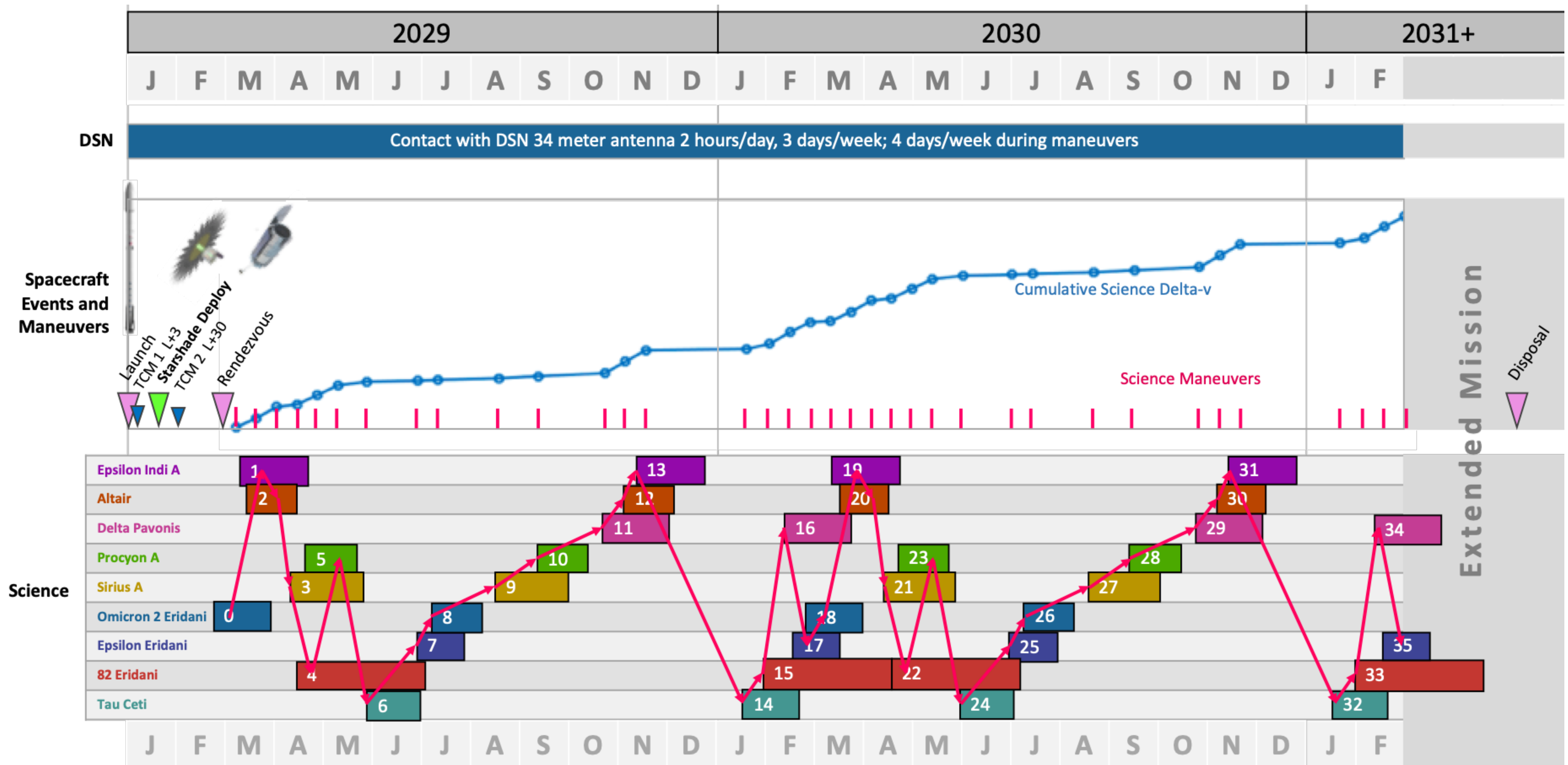

Mission Timeline

Red line segments are slews (2 days to 2 weeks)

Red dots: single day's observation

Horizontal bars: target star observability windows based on Sun angular constraints

Courtesy Doug Lisman

Optimized Mission Planning – EXOSIMS

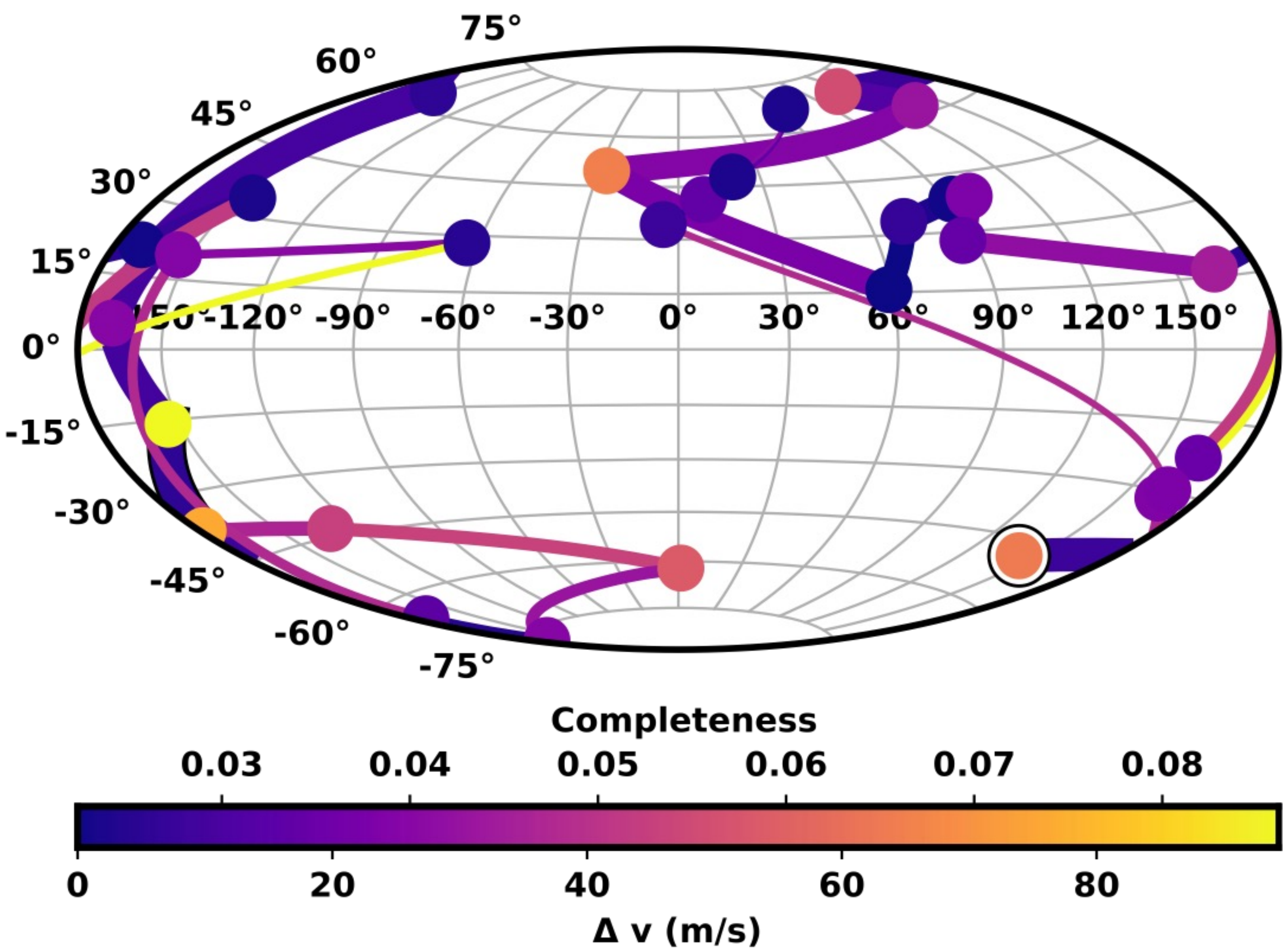

Monte Carlo simulation accounting for optimal integration times, fuel use, retargeting time, and keep out zones to balance completeness, spectroscopy, revisits, and number of targets.

Soto, et al., 2019

4 m telescope - Example Yield Results

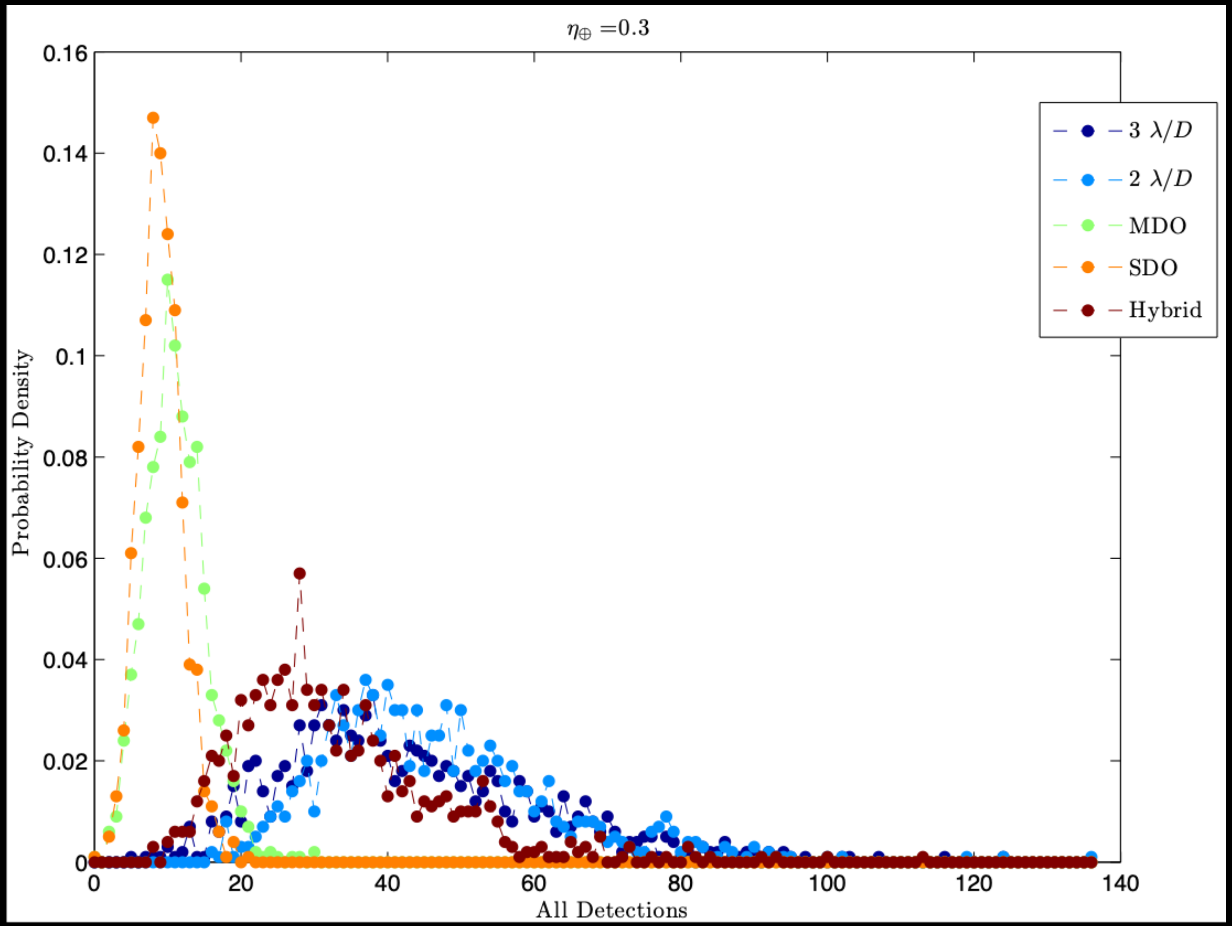

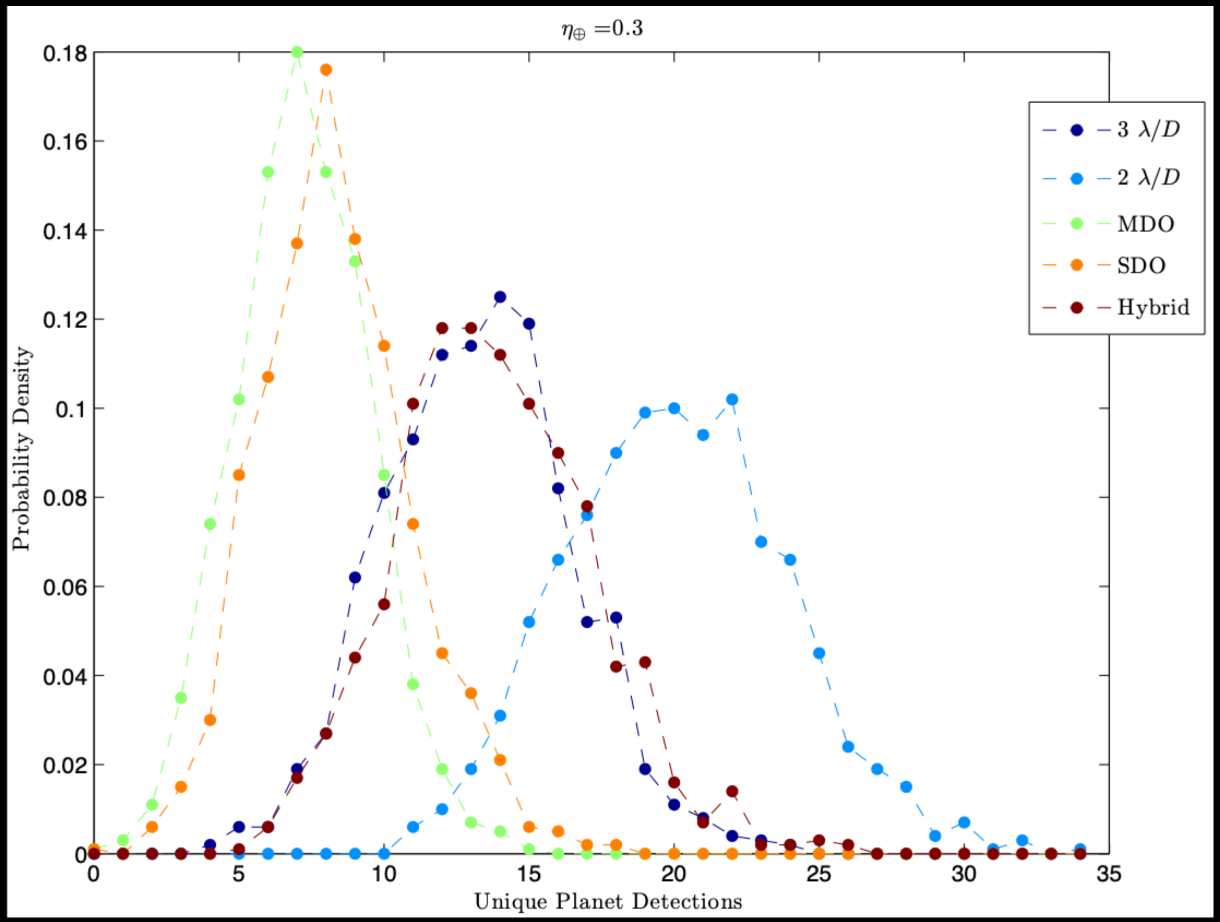

Sample comparison of probability distributions of detecting an Earth using a coronagraph with IWA of 2 and 3 lambda/D, a multi- and single-distance starshade and a hybrid mission with both coronagraph and star shade (such as HabEx) with a 4 m telescope.

Savransky 2010

4 m telescope - Full and Partial Spectra

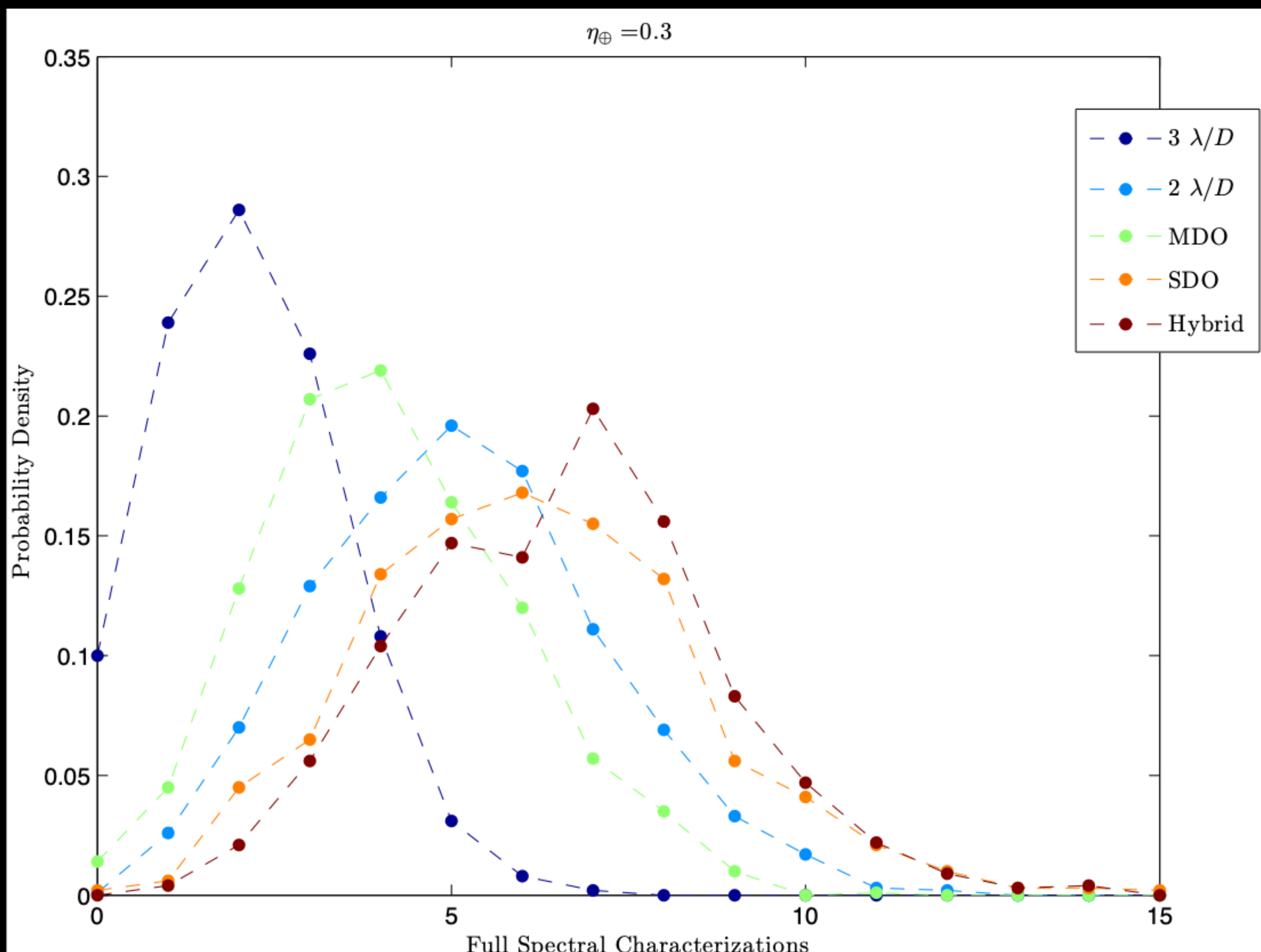

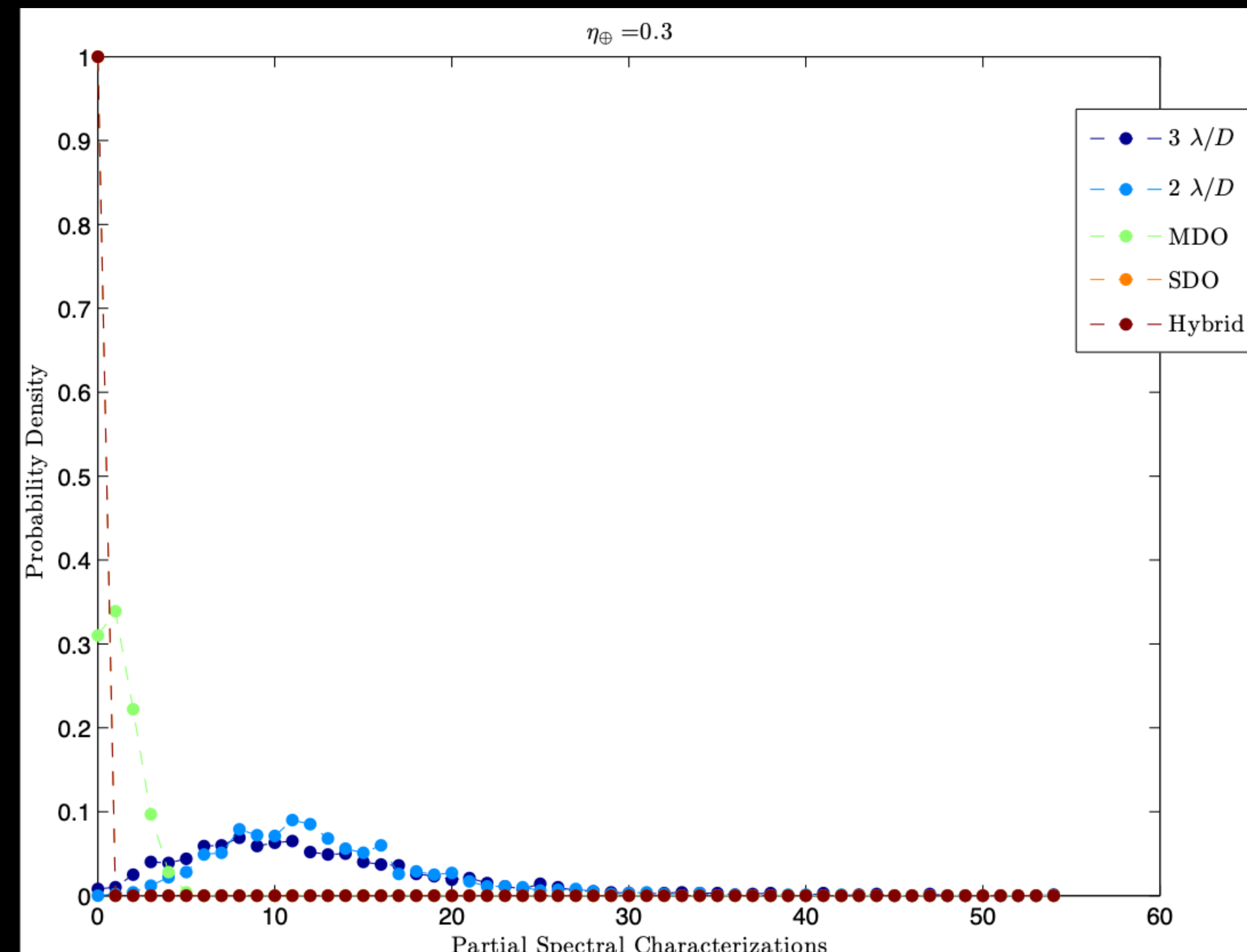

- 2 l/D coronagraph is necessary to get any spectra
- 3 l/d has non-negligible probability of zero planets.
- Number of full spectra for coronagraph limited by red end (1000 nm)
- SDO & MDO close in performance
- Hybrid best performance but assumes 3 l/D coronagraph is possible

Thank You